

Fracton physics of spatially extended excitations. II. Polynomial ground state degeneracy of exactly solvable models

Meng-Yuan Li and Peng Ye*

*School of Physics and State Key Laboratory of Optoelectronic Materials and Technologies,
Sun Yat-sen University, Guangzhou, 510275, China*

(Dated: Tuesday 14th December, 2021)

Generally, “fracton” topological orders are referred to as gapped phases that support *point-like topological excitations* whose mobility is, to some extent, restricted. In our previous work [[Phys. Rev. B 101, 245134 \(2020\)](#)], a large class of exactly solvable models on hypercubic lattices are constructed. In these models, *spatially extended excitations* possess generalized fracton-like properties: not only mobility but also deformability is restricted. As a series work, in this paper, we proceed further to compute ground state degeneracy (GSD) in both isotropic and anisotropic lattices. We decompose and reconstruct ground states through a consistent collection of subsystem ground state sectors, in which mathematical game “coloring method” is applied. Finally, we are able to systematically obtain GSD formulas (expressed as $\log_2 GSD$) which exhibit diverse kinds of polynomial dependence on system sizes. For example, the GSD of the model labeled as $[0, 1, 2, 4]$ in four dimensional isotropic hypercubic lattice shows $12L^2 - 12L + 4$ dependence on the linear size L of the lattice. Inspired by existing results [[Phys. Rev. X 8, 031051 \(2018\)](#)], we expect that the polynomial formulas encode geometrical and topological fingerprints of higher-dimensional manifolds beyond toric manifolds used in this work. This is left to future investigation.

CONTENTS

| | | | |
|--|----|--|----|
| I. Introduction | 1 | VI. Discussions and Conclusions | 13 |
| II. Preliminaries | 2 | Acknowledgements | 14 |
| A. Geometric notations | 2 | A. Notations and conventions | 14 |
| B. Review of $[d_n, d_s, d_l, D]$ models | 4 | B. Proof of the isomorphism between ground states and consistent combinations of SGS's | 15 |
| III. Representing ground states with lower-dimensional data | 6 | References | 15 |
| A. Decomposition of lattices | 6 | | |
| B. Decomposition of Ising configurations and quantum operators | 7 | | |
| C. Subsystem ground state sector (SGS) as a holographic shadow of ground states | 7 | | |
| D. Application in $[0, 1, 2, 3]$ model (X-cube model) | 8 | | |
| IV. General procedures and coloring method | 9 | | |
| A. General procedures | 9 | | |
| B. Coloring method: general description and application in $[0, 1, 2, 3]$ model (i.e., X-cube model) | 9 | | |
| V. Typical examples | 11 | | |
| A. GSD of $[0, 1, 2, D]$ models on isotropic lattices | 11 | | |
| B. GSD of $[0, 1, 2, D]$ models on anisotropic lattices | 12 | | |
| C. GSD of $[D - 3, D - 2, D - 1, D]$ models on isotropic lattices | 12 | | |
| D. GSD of $[D - 3, D - 2, D - 1, D]$ models on anisotropic lattices | 13 | | |

I. INTRODUCTION

Topological orders are gapped phases of matter that cannot be characterized by symmetry-breaking order parameters and are robust without the need of symmetry protection [1]. To characterize topological orders, topological order parameters, such as braiding statistics and ground state degeneracy (GSD) are applied to characterize topological orders, as long as the bulk gap is not closed [2, 3]. Recently, a new kind of orders, dubbed *fracton (topological) order*, has been drawing much attention [4–54]. Fracton orders exhibit an interesting interplay of topology and geometry in quantum many-body physics. One of remarkable topological properties is the restricted mobility of topological excitations. More precisely, topological excitations in disorder-free fracton order systems cannot be moved away from their initial locations by local operators or more general local noise. In the extreme case where mobility towards all spatial directions is entirely frozen, such a kind of topological excitations is dubbed “fracton” following nomenclature widely used in the literature. The remaining excitations are “subdimensional particles” that have partial mobility and are thus movable within certain subspaces. Such a restriction on mobility of excitations is essentially rooted in topological

* yepeng5@mail.sysu.edu.cn

reasons, which becomes crystal clear in exactly solvable model construction in terms of stabilizer codes [12]. Recently, there have been multidisciplinary research activities in quantum information, condensed matter physics, and high energy physics, e.g., fragmentation of Hilbert space, robust storage of quantum memory, new duality, gravity, and higher rank gauge theory.

In the literature, most of exactly solvable models of fracton orders only contain *point-like* topological excitations with restricted mobility. Nevertheless, in 3D and higher-dimensional pure topological orders, we have been witnesses to ongoing research progress on fruitful physics of spatially extended topological excitations, such as strings and membranes [55–80]. Therefore, it is fundamentally important to explore fracton-type physics of spatially extended excitations. For this goal, in the work [50], we proposed a series of exactly solvable lattice models that are uniquely labeled by a group of four integers: $[d_n, d_s, d_l, D]$. Here, D means D -dimensional cubic lattice. To our surprise, these models contain not only point-like subdimensional excitations, but also spatially extended excitations whose mobility and deformability are restricted to some extent. Besides, we construct spatially extended excitations with stable non-manifold-like shapes, which are termed “complex excitations”. Excitations with stable disconnected shapes are also discussed. In conclusion, we classify topological excitations into 4 sectors, which are respectively trivial, simple, disconnected and complex excitations.

In conventional topological orders, GSD depends on topology of base manifolds where many-body systems are spatially defined, and cannot be lifted by local operators in the thermodynamical limit. In fracton orders, GSD is also robust against local operators and ground states are indistinguishable from each other via local measurements. But GSD of fracton orders is no longer uniquely determined by topology of base manifolds. Rather, GSD quantitatively depends on various topological and geometric properties, such as foliation and boundary conditions [6, 7, 10–12, 18, 19, 81–83]. For example, GSD of fracton orders in the X-cube model exponentially explodes with respect to the linear size L of the system, i.e., $GSD \sim 2^{6L-3}$. In the literature, the coefficients of linear terms of $\log_2 GSD$ have been identified as the first Betti numbers with \mathbb{Z}_2 coefficients of leaves [18], which opens a new condensed-matter window into mathematics. In short, GSD is a very important topological order parameter, and also a significant character that explicitly distinguishes fracton orders from conventional topological orders.

As a series work, in this paper, we move forward and study GSD of $[d_n, d_s, d_l, D]$ models constructed in Ref. [50]. As an initial attempt, we present a combinatorial method to rigorously derive GSD formulas of a subset of $[d_n, d_s, d_l, D]$ models, which are summarized in Table. I. Our results show that GSD values are expressed as diverse kinds of polynomial dependence on the linear sizes of both isotropic and anisotropic hyper-

cubic lattices. As we shall discuss in the main text, the polynomial expressions of $\log_2 GSD$ of $[0, 1, 2, D]$ models are fundamentally rooted in exotic multi-level foliation structures of the models ($D \geq 4$). *Here, multi-level foliation means that a ground state of a $[0, 1, 2, D]$ model restricted in a $(D - 1)$ -dimensional subspace is a $[0, 1, 2, D - 1]$ ground state which again exhibits a foliation structure.* A comprehensive discussion on restriction of ground states will be given in Sec. III. Inspired by elegant results in Ref. [18], we expect these polynomials may potentially encode rich mathematics of topology and geometry, which will be one of appealing future directions.

To obtain GSD formulas, we technically perform an exotic decomposition of base manifolds for $[d_n, d_s, d_l, D]$ models, which can be intuitively recognized as a class of foliation structures of different dimensions. Accordingly, we also need to decompose Ising configurations (in spin- z basis), stabilizers and ground states of $[d_n, d_s, d_l, D]$ models. By proving that there is a one-to-one correspondence between a ground state sector in the fracton ordered model and a consistent collection of subsystem ground state sectors, we finally obtain GSD with a combinatorial algorithm. The latter is an interesting math game: coloring method.

This paper is organized as follows. In Sec. II, we introduce some useful preliminary materials that are critical to our proof and computation. In Sec. III, we present the details of representing ground states with lower-dimensional data. With the preparations in the former two sections, Sec. IV is devoted to the general steps toward the ground state degeneracy. In Sec. V, we demonstrate the calculation of GSD of some typical $[d_n, d_s, d_l, D]$ models following the general steps. In Sec. VI, we give a brief summary of our computation of GSD and potential implications, and tentatively discuss about some relevant questions yet to be solved. There are also two useful appendix at the end of the paper.

II. PRELIMINARIES

A. Geometric notations

To refer to objects of all dimensions, it is useful to introduce a series of geometric notations. We begin with an introduction of a coordinate system. In this paper, as we mainly focus on cubic lattice, we can refer to a *d-cube* denoted as γ_d via the coordinate of its geometric center. Here a *d-cube* is a d -dimensional analog of a cube¹. Furthermore, by setting the lattice constant to be 1, the coordinate of a d -cube in a D -dimensional cubic lattice always contains $(D - d)$ integers and d half-integers. For example, in a 3-dimensional cubic lattice, $(0, 0, 0)$ refers

¹ For example, 0-cubes are vertices, 1-cubes are links, and 2-cubes are plaquettes.

TABLE I. **Ground state degeneracy (GSD) results of $[d_n, d_s, d_l, D]$ models on both isotropic and anisotropic lattices with periodic boundary conditions (PBC).** GSD as a function of L is computed in isotropic lattices with linear size L . Otherwise, GSD is computed in anisotropic lattices, where L_n is the linear size along the \hat{x}_n direction of lattices. It is known that in X-cube model, the coefficients of the linear terms are the first Betti numbers of leaves. Therefore, these coefficients reflect the topological properties of leaves. While as we can see, in $[0, 1, 2, D]$ models with $D \geq 4$, except for the linear term, we also obtain terms of higher degrees. Moreover, in anisotropic models, there are also crossing terms between sizes along different directions. Such terms of higher degrees call for further investigation on their relations to topological and geometric properties of the models.

| Model | $\log_2 \text{GSD}$ |
|----------------------|--|
| X-cube | $6L - 3$ |
| $[0, 1, 2, 4]$ | $12L^2 - 12L + 4$ |
| $[1, 2, 3, 4]$ | $12L - 6$ |
| $[0, 1, 2, D]$ | $\sum_{n=0}^{D-2} D \times \binom{D-1}{n} (-1)^{D+n} L^n$ |
| $[D-3, D-2, D-1, D]$ | $\binom{D}{D-2} \times (2L - 1)$ |
| X-cube | $2L_1 + 2L_2 + 2L_3 - 3$ |
| $[0, 1, 2, 4]$ | $2 \sum_{i < j} L_i L_j - 3 \sum_i L_i + 4$ |
| $[1, 2, 3, 4]$ | $3L_1 + 3L_2 + 3L_3 + 3L_4 - 6$ |
| $[0, 1, 2, 5]$ | $2 \sum_{i < j < k} L_i L_j L_k - 3 \sum_{i < j} L_i L_j + 4 \sum_i L_i - 5$ |
| $[2, 3, 4, 5]$ | $4L_1 + 4L_2 + 4L_3 + 4L_4 + 4L_5 - 10$ |

to a 0-cube, i.e., a point $(0, 0, 0)$; $(\frac{1}{2}, 0, 0)$ refers to a 1-cube, i.e., a link whose center is $(\frac{1}{2}, 0, 0)$; $(\frac{1}{2}, \frac{1}{2}, 0)$ refers to a 2-cube, i.e., a plaquette whose center is $(\frac{1}{2}, \frac{1}{2}, 0)$; $(\frac{1}{2}, \frac{1}{2}, \frac{1}{2})$ refers to a 3-cube, i.e., a common cube whose center is $(\frac{1}{2}, \frac{1}{2}, \frac{1}{2})$.

Next, we explain the meaning of “nearest to”. In a D -dimensional cubic lattice, for $\gamma_{d_i} = (x_1, x_2, \dots, x_D)$ and $\gamma_{d_j} = (y_1, y_2, \dots, y_D)$, we say they are nearest to each other if and only if:

$$\begin{aligned}
 L_1(\gamma_{d_i}, \gamma_{d_j}) &\equiv |x_1 - y_1| + |x_2 - y_2| + \dots + |x_D - y_D| \\
 &= \frac{|d_i - d_j|}{2}, \quad (d_i \neq d_j), \\
 L_1(\gamma_{d_i}, \gamma_{d_j}) &\equiv |x_1 - y_1| + |x_2 - y_2| + \dots + |x_D - y_D| \\
 &= 1, \quad (d_i = d_j).
 \end{aligned}$$

Moreover, given $d_i < d_j$, γ_{d_i} being inside γ_{d_j} is equivalent to that γ_{d_i} being nearest to γ_{d_j} . A more detailed introduction of this notation is given in Sec. II of Ref. [50].

Furthermore, in order to give an intuitive picture of the definition of $[d_n, d_s, d_l, D]$ models, here we give a heuristic introduction of foliation. For a more detailed discussion, see Ref. [84]. In general, foliation is the partition of a manifold into a set of submanifolds, where each submanifold is dubbed “leaf”. For a regular foliation, where all leaves are of the same dimension, the dimension of leaves is defined as the dimension of the foliation. In this paper, as we only consider lattices defined on toric manifolds and regular foliations, we will treat leaves simply as sublattices. An example of foliation is pictorially illustrated in Fig. 1. For foliated fracton orders, two systems belong to the same phase if they can be transformed to each other under addition or removal of subdimensional topologically ordered phases. Therefore, their physical properties, like ground state degeneracy, have direct relationship with their foliation struc-

tures. A large amount of type-I fracton orders have been proved to be foliated fracton orders, like X-cube model and checkerboard model [10, 11, 85].

Last but not least, inspired by the idea of higher-order topological insulator [86], here we give a rough definition of higher-order boundary in cubic and hypercubic lattices, in order to refer to the higher-dimensional analogs of hinges of a cuboid. Firstly, we consider the d -dimensional analogs of cuboid, denoted as S^d . For example, an S^1 is a straight string, an S^2 is a flat membrane, and an S^3 is a cuboid². See Ref. [50] for more details of S^n notations. Then, for such an S^d , we can define its d_i -dimensional boundary as follows (here $d_i < d$ is assumed):

- The d_i -dimensional boundary of an S^d is composed of γ_{d_i} ’s.
- A γ_{d_i} belongs to the d_i -dimensional boundary of the S^d if and only if it is nearest to exactly one γ_d in the S^d .

We can check that such a definition is consistent with our intuition. For example, the 0-dimensional boundary of a plaquette is composed of the 4 vertices of the plaquette, and the 1-dimensional boundary of a common cube is composed of the 12 hinges of the cube. While for a cuboid extended along one spatial direction, we can see that its 1-dimensional boundary is composed of only 4 hinges.

² Here it is important to notice that S^d is always “flat”. For example, an “L”-shaped string is composed of 2 S^1 ’s, and the turning point of the string should be recognized as a vertex emanating 2 perpendicular S^1 ’s

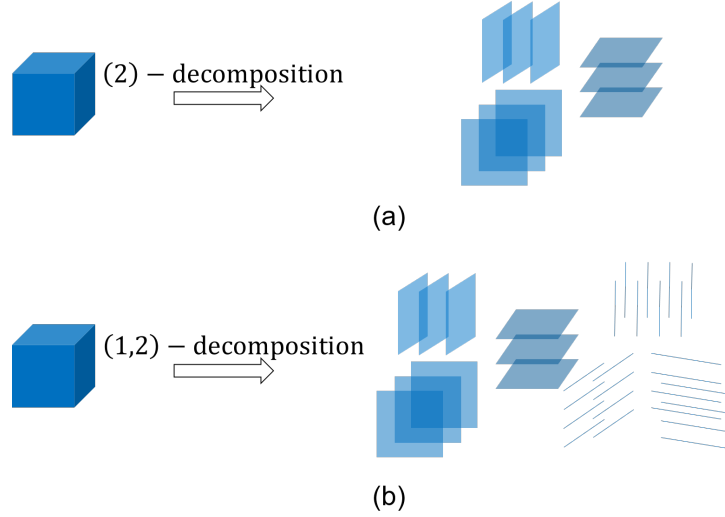


FIG. 1. **Decompositions of 3-torus for X-cube model, where spins are located on links.** As we can see, while the decomposition in (a) shows a regular 2-dimensional foliation of the original 3-manifold, the decomposition in (b) additionally gives a foliation structure to each 2-dimensional leaf space in (a).

B. Review of $[d_n, d_s, d_l, D]$ models

As we shall exemplify our GSD computing algorithm with the $[d_n, d_s, d_l, D]$ models proposed in Ref. [50], it would be beneficial to give a review of the definition of the models at first. $[d_n, d_s, d_l, D]$ models are defined on D -dimensional cubic lattice with $1/2$ -spins as basic degrees of freedom. There is a spin (i.e., a qubit) at the center of each γ_{d_s} . The Hamiltonian is defined as below:

$$H_{[d_n, d_s, d_l, D]} = -J \sum_{\{\gamma_D\}} A_{\gamma_D} - K \sum_{\{\gamma_{d_n}\}} \sum_l B_{\gamma_{d_n}}^l, \quad (1)$$

where $J, K > 0$ are coupling constants. $d_n < d_s < d_l < D$ is assumed. Apparently, there are two typical terms in the Hamiltonian, namely, A -term and B -term.

- First, given a γ_D , the Hermitian operator A_{γ_D} is the product of all x -components (i.e., σ^x) of spins whose corresponding γ_{d_s} 's are nearest to the γ_D . The definition of “nearest to” can be found in Sec. II A.
- Second, in order to determine the $B_{\gamma_{d_n}}^l$ term, we need to choose a d_l -dimensional sublattice l in which the γ_{d_n} cube is embedded³. Then we need to find all γ_{d_s} 's which are not only nearest to the γ_{d_n} but also totally embedded in l . Then $B_{\gamma_{d_n}}^l$ is just

the product of the z -components of all the spins at the centers of such d_s -cubes.

We note that, in general, there are infinite “parallel” sublattices if we only specify d_l orthogonal directions. But the requirement of “ γ_{d_n} being embedded in the sublattice” unambiguously leads to a unique sublattice. Therefore, we only need to give d_l orthogonal directions that unambiguously constitute the label l . For example, in X-cube model, where $d_l = 2$, we use $\langle \hat{x}_1 \hat{x}_2 \rangle$, $\langle \hat{x}_1 \hat{x}_3 \rangle$ and $\langle \hat{x}_2 \hat{x}_3 \rangle$ as the superscripts of B terms. See Eq. (2) for an instance.

According to the definition of Hamiltonians, we can see that the numbers in the label of a $[d_n, d_s, d_l, D]$ model are just dimension indices. In Ref. [50], it has been proved that a $[d_n, d_s, d_l, D]$ model is exactly solvable when d_n, d_s, d_l and D satisfy $(d_l - d_n) \bmod 2 = 0$ together with $d_n < d_s < d_l < D$. Among them, there are two specially interesting branches of such exactly solvable models, $[0, 1, 2, D]$ and $[D - 3, D - 2, D - 1, D]$. In this paper, we will mainly focus on these two branches of models.

In $[D - 3, D - 2, D - 1, D]$ models with $D \geq 4$, our previous work [50] demonstrates that there are extended excitations with fracton physics. That is to say, both mobility and deformability of spatially extended excitations (e.g. loop excitations and membrane excitations) in these models can be restricted. What is more, some topological excitations can even have non-manifold shapes. Such excitations with non-manifold-like shapes are dubbed “complex excitations”. For complex excitations, as long as the connectivity of their shapes is preserved, they cannot be deformed to be manifold-like objects by any local unitary operators. Similarly, we can also define (intrinsically) disconnected excitations, whose shapes cannot be deformed to be connected by any local

³ By “sublattice”, we mean that the sublattice is a part of the whole D -dimensional cubic lattice in the usual sense. For example, a flat plane formed by plaquettes is a $d_l=2$ sublattice. By “embed”, we mean that the γ_{d_n} cube is exactly an ingredient of the sublattice.

unitary operators. In conclusion, topological excitations in $[d_n, d_s, d_l, D]$ models can be classified into 4 sectors, which are respectively trivial excitations, simple excitations, disconnected excitations and complex excitations. The latter 2 sectors only exist in fracton orders.

Following the aforementioned rules of construction of Hamiltonians, we express explicitly Hamiltonians of some models when $D = 3, 4$:

- **X-cube model (i.e., $[0, 1, 2, 3]$ model)** In our notation, X-cube model is denoted as $[0, 1, 2, 3]$. Thus, $d_n = 0$, $d_s = 1$, $d_l = 2$ and $D = 3$. Since $d_s = 1$, spins are located at the centers of links. The Hamiltonian is composed of $B_{\gamma_0}^l$ and A_{γ_3} terms defined on vertices and cubes respectively. And since we have $d_l = 2$, such a $B_{\gamma_0}^l$ term equals to the product of 4 σ^z 's sitting on the 4 links which are (a) embedded in the plane l and (b) nearest to the vertex γ_0 . Similarly, an A_{γ_3} term is the product of 12 σ^x 's sitting on the 12 links that are nearest to the γ_3 . For example, for a common cubic lattice, we have

$$B_{(0,0,0)}^{\langle \hat{x}_1, \hat{x}_2 \rangle} = \sigma_{(0, \frac{1}{2}, 0)}^z \sigma_{(-\frac{1}{2}, 0, 0)}^z \sigma_{(\frac{1}{2}, 0, 0)}^z \sigma_{(0, -\frac{1}{2}, 0)}^z, \quad (2)$$

and

$$A_{(\frac{1}{2}, \frac{1}{2}, \frac{1}{2})} = \sigma_{(0, 0, \frac{1}{2})}^x \sigma_{(0, 1, \frac{1}{2})}^x \sigma_{(1, 0, \frac{1}{2})}^x \sigma_{(1, 1, \frac{1}{2})}^x \sigma_{(0, \frac{1}{2}, 0)}^x \sigma_{(0, \frac{1}{2}, 1)}^x \sigma_{(1, \frac{1}{2}, 0)}^x \sigma_{(1, \frac{1}{2}, 1)}^x \sigma_{(\frac{1}{2}, 0, 0)}^x \sigma_{(\frac{1}{2}, 0, 1)}^x \sigma_{(\frac{1}{2}, 1, 0)}^x \sigma_{(\frac{1}{2}, 1, 1)}^x, \quad (3)$$

where subscript coordinates like $(0, 0, 0)$ and $(1, 0, \frac{1}{2})$ respectively refer to a γ_0 and a γ_1 , as they are exactly the geometric centers of these two objects. In X-cube model, we have fractons and lineons as fundamental excitations. These excitations respectively correspond to the eigenvalue flips of A_{γ_3} and $B_{\gamma_0}^l$ terms.

Here we also give a brief introduction of the ground states of X-cube model (for a more detailed review of X-cube model, see Ref. [4, 5]). As a stabilizer code model, a ground state of X-cube model $|\phi\rangle$ should satisfy the following conditions:

$$B_{\gamma_0}^l |\phi\rangle = |\phi\rangle, \quad \forall \gamma_0, l; \quad A_{\gamma_3} |\phi\rangle = |\phi\rangle, \quad \forall \gamma_3.$$

Hence, in σ^z basis, such a ground state $|\phi\rangle$ must be an equal weight superposition of S^1 's (i.e. straight strings) with vertices emanating 3 perpendicular S^1 's. Similar to toric code model, independent ground states of X-cube model can be distinguished by the action of non-local logical operator $W(S^1) = \prod_{\gamma_1 \in S^1} \sigma_{\gamma_1}^x$ with non-contractible S^1 . Besides, in X-cube model, four S^1 's that compose the 1-dimensional boundary of an S^3 extended in one direction can be created or annihilated by applying A_{γ_3} stabilizers. From another perspective, it means that one single non-local string can be "split" to 3 different non-local strings under the action of A_{γ_3} stabilizers.

- **$[0, 1, 2, 4]$ model** The Hamiltonian of $[0, 1, 2, 4]$ model is composed of $B_{\gamma_0}^l$ and A_{γ_4} terms. And since we have $d_l = 2$, such a $B_{\gamma_0}^l$ term equals to the product of 4 σ^z 's sitting on the 4 links which are (a) embedded in the plane l and (b) nearest to the vertex γ_0 . Similarly, an A_{γ_4} term is the product of 32 σ^x 's sitting on the 32 links that are nearest to the γ_4 . For a common hypercubic lattice, we have

$$B_{(0,0,0,0)}^{\langle \hat{x}_1, \hat{x}_2 \rangle} = \sigma_{(0, \frac{1}{2}, 0, 0)}^z \sigma_{(-\frac{1}{2}, 0, 0, 0)}^z \sigma_{(\frac{1}{2}, 0, 0, 0)}^z \sigma_{(0, -\frac{1}{2}, 0, 0)}^z, \quad (4)$$

and

$$A_{(\frac{1}{2}, \frac{1}{2}, \frac{1}{2}, \frac{1}{2})} = \sigma_{(0, 0, \frac{1}{2}, 0)}^x \sigma_{(0, 1, \frac{1}{2}, 0)}^x \sigma_{(1, 0, \frac{1}{2}, 0)}^x \sigma_{(1, 1, \frac{1}{2}, 0)}^x \sigma_{(0, \frac{1}{2}, 0, 0)}^x \sigma_{(0, \frac{1}{2}, 1, 0)}^x \sigma_{(1, \frac{1}{2}, 0, 0)}^x \sigma_{(1, \frac{1}{2}, 1, 0)}^x \sigma_{(\frac{1}{2}, 0, 0, 0)}^x \sigma_{(\frac{1}{2}, 0, 1, 0)}^x \sigma_{(\frac{1}{2}, 1, 0, 0)}^x \sigma_{(\frac{1}{2}, 1, 1, 0)}^x \sigma_{(0, 0, \frac{1}{2}, 1)}^x \sigma_{(0, 1, \frac{1}{2}, 1)}^x \sigma_{(1, 0, \frac{1}{2}, 1)}^x \sigma_{(1, 1, \frac{1}{2}, 1)}^x \sigma_{(0, \frac{1}{2}, 0, 1)}^x \sigma_{(0, \frac{1}{2}, 1, 1)}^x \sigma_{(1, \frac{1}{2}, 0, 1)}^x \sigma_{(1, \frac{1}{2}, 1, 1)}^x \sigma_{(\frac{1}{2}, 0, 0, 1)}^x \sigma_{(\frac{1}{2}, 0, 1, 1)}^x \sigma_{(\frac{1}{2}, 1, 0, 1)}^x \sigma_{(\frac{1}{2}, 1, 1, 1)}^x \sigma_{(0, 0, 0, \frac{1}{2})}^x \sigma_{(0, 0, 1, \frac{1}{2})}^x \sigma_{(0, 1, 0, \frac{1}{2})}^x \sigma_{(0, 1, 1, \frac{1}{2})}^x \sigma_{(1, 0, 0, \frac{1}{2})}^x \sigma_{(1, 0, 1, \frac{1}{2})}^x \sigma_{(1, 1, 0, \frac{1}{2})}^x \sigma_{(1, 1, 1, \frac{1}{2})}^x. \quad (5)$$

In $[0, 1, 2, 4]$ model, we have fractons and lineons as fundamental excitations. These excitations respectively correspond to the eigenvalue flips of A_{γ_4} and $B_{\gamma_0}^l$ terms. A pictorial demonstration of such an A_{γ_4} term is given in Fig. 2.

- **$[1, 2, 3, 4]$ model** The Hamiltonian of $[1, 2, 3, 4]$ model is composed of $B_{\gamma_1}^l$ and A_{γ_4} terms. And since we have $d_l = 3$, such a $B_{\gamma_1}^l$ term equals to the product of 4 σ^z 's sitting on the 4 plaquettes which are (a) embedded in the 3-dimensional space l and (b) nearest to the link γ_1 . Similarly, an A_{γ_4} term is the product of 24 σ^x 's sitting on the 24 plaquettes that are nearest to the γ_4 . For a common hypercubic lattice, we have

$$B_{(0,0,0,\frac{1}{2})}^{\langle \hat{x}_1, \hat{x}_2, \hat{x}_4 \rangle} = \sigma_{(\frac{1}{2}, 0, 0, \frac{1}{2})}^z \sigma_{(-\frac{1}{2}, 0, 0, \frac{1}{2})}^z \sigma_{(0, \frac{1}{2}, 0, \frac{1}{2})}^z \sigma_{(0, -\frac{1}{2}, 0, \frac{1}{2})}^z, \quad (6)$$

and

$$A_{(\frac{1}{2}, \frac{1}{2}, \frac{1}{2}, \frac{1}{2})} = \sigma_{(0, 0, \frac{1}{2}, \frac{1}{2})}^x \sigma_{(0, 1, \frac{1}{2}, \frac{1}{2})}^x \sigma_{(1, 0, \frac{1}{2}, \frac{1}{2})}^x \sigma_{(1, 1, \frac{1}{2}, \frac{1}{2})}^x \sigma_{(0, \frac{1}{2}, 0, \frac{1}{2})}^x \sigma_{(0, \frac{1}{2}, 1, \frac{1}{2})}^x \sigma_{(1, \frac{1}{2}, 0, \frac{1}{2})}^x \sigma_{(1, \frac{1}{2}, 1, \frac{1}{2})}^x \sigma_{(0, \frac{1}{2}, \frac{1}{2}, 0)}^x \sigma_{(0, \frac{1}{2}, \frac{1}{2}, 1)}^x \sigma_{(1, \frac{1}{2}, \frac{1}{2}, 0)}^x \sigma_{(1, \frac{1}{2}, \frac{1}{2}, 1)}^x \sigma_{(\frac{1}{2}, 0, 0, \frac{1}{2})}^x \sigma_{(\frac{1}{2}, 0, 1, \frac{1}{2})}^x \sigma_{(\frac{1}{2}, 1, 0, \frac{1}{2})}^x \sigma_{(\frac{1}{2}, 1, 1, \frac{1}{2})}^x \sigma_{(\frac{1}{2}, 0, \frac{1}{2}, 0)}^x \sigma_{(\frac{1}{2}, 0, \frac{1}{2}, 1)}^x \sigma_{(\frac{1}{2}, 1, \frac{1}{2}, 0)}^x \sigma_{(\frac{1}{2}, 1, \frac{1}{2}, 1)}^x \sigma_{(\frac{1}{2}, \frac{1}{2}, 0, 0)}^x \sigma_{(\frac{1}{2}, \frac{1}{2}, 0, 1)}^x \sigma_{(\frac{1}{2}, \frac{1}{2}, 1, 0)}^x \sigma_{(\frac{1}{2}, \frac{1}{2}, 1, 1)}^x. \quad (7)$$

In $[1, 2, 3, 4]$ model, we have fractons and $(1, 2)$ -type excitations as fundamental excitations. These

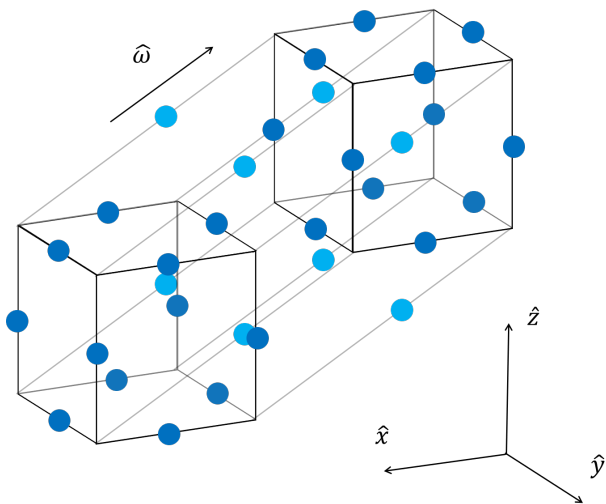


FIG. 2. **Pictorial demonstration of an A_{γ_4} term in $[0, 1, 2, 4]$ model on a 4-dimensional lattice.** Spins are located on links, and they are represented by blue dots. While for clarity, spins along the fourth spatial dimension denoted as $\hat{\omega}$ are highlighted with light blue. As we can see, the A_{γ_4} is the product of 32 σ^x operators on the 32 links of a 4-dimensional hypercube.

excitations respectively correspond to the eigenvalue flips of A_{γ_4} and $B_{\gamma_1}^l$ terms. Here (1, 2)-type means that the excitation is intrinsically 1-dimensional (i.e. it is a string), and its mobility and deformability are restricted in a 2-dimensional subspace. For more details of (m, n) -type excitations, see Ref. [50].

What is more, in $[1, 2, 3, 4]$ model, there are also complex excitations *chairon* and *yuon*, whose shapes are non-manifold-like. As an example, the shape of a yuon is composed of 3 strings which share one pair of endpoints. Due to the deformability restriction, such a non-manifold shape of a yuon is invariant under local unitary transformations, as long as its connectivity is preserved.

III. REPRESENTING GROUND STATES WITH LOWER-DIMENSIONAL DATA

As we are trying to compute the GSD of a $[d_n, d_s, d_l, D]$ model by data from lower-dimensional subsystems⁴, it is important to define the subsystem structures strictly. So in this section, we will introduce the definition of decomposition and restriction of lattices, Ising configurations, and ground states. And finally, we prove that in certain cases, there is a one-to-one correspondence between a collection of subsystem ground state sectors (SGS) satisfying certain *consistent conditions* (to be defined in

this section) and a ground state of the original system. Consequently, it is plausible to compute the GSD of a $[d_n, d_s, d_l, D]$ model by counting the number of possible combinations of subsystem states.

A. Decomposition of lattices

To define a decomposition of a ground state in a general $[d_n, d_s, d_l, D]$ model, we find that it is necessary to first consider a decomposition of manifolds. More concretely, because the “ground state degeneracy” of a leaf can also be subextensive, in some higher-dimensional models, we can consider “leaves of a leaf.” From another view, a higher-dimensional $[d_n, d_s, d_l, D]$ model may admit foliation structures of various dimensions. As a result, we believe it is beneficial to define a “decomposition” of the base manifold. Besides, in this paper, as we are mainly interested in lattice models, manifolds are always assumed to be equipped with a lattice structure (i.e., cellulation) given by the definition of a $[d_n, d_s, d_l, D]$ model. *Therefore, when the lattice structure is specified, we will alternatively use “(sub-)lattice” and “(sub-)manifold”. For simplicity, in the paper we only consider toric base manifolds.*

For a base manifold M^D , we define a (d_1, d_2, \dots, d_k) -decomposition (denoted by \mathcal{M}) as a collection composed of sets of lower-dimensional manifolds

$$\mathcal{M} \equiv \{M^{d_1}\} \cup \{M^{d_2}\} \cup \dots \cup \{M^{d_k}\}, \quad (8)$$

where the notation $\{M^{d_i}\}$ denotes a set in which all manifolds are d_i -dimensional. The above definition of decomposition, i.e., Eq. (8) satisfies the following (without loss of generality, we always assume $d_1 < d_2 < \dots < d_k$):

- For any $\{M^{d_i}\}$, we have $\cup_{M \in \{M^{d_i}\}} M = M^D$. Specially, for lattices, this condition requires that every spin belongs to at least one sublattice $M \in \{M^{d_i}\}, \forall d_i$.
- For any two sets of lower-dimensional manifolds $\{M^{d_i}\}$ and $\{M^{d_j}\}$ with $d_i < d_j$, we require that for any $M^{d_j} \in \{M^{d_j}\}$, there exists a subset $\{\tilde{M}^{d_i}\} \subset \{M^{d_i}\}$, such that $\cup_{M^{d_i} \in \{\tilde{M}^{d_i}\}} M^{d_i} = M^{d_j}$. For lattices, this condition requires that every spin in M^{d_j} belongs to at least one sublattice $M^{d_i} \in \{\tilde{M}^{d_i}\}$.

Here, it should be noted that these conditions show that a decomposition of a manifold equipped with a lattice structure can only be determined when the $[d_n, d_s, d_l, D]$ model is specified. The reason is rather obvious: specifying a model can tell how spins (qubits) are distributed spatially. In the simplest decomposition, the collection \mathcal{M} contains only subsystems of the same dimension, i.e., $\mathcal{M} = \{M^{d_i}\}$ with $d_i < D$, a regular foliation of M^D is achieved [84]. When the collection contains sets of sublattices of different dimensions, the decomposition gives foliation structures with different dimensional sublattices, too (see Fig. 1).

⁴ In this paper, we use “sublattice” and “subsystem” alternatively.

In this paper, as we do not discuss about the influence of the topology of sublattices in detail, we always assume that the decompositions are isotropic and composed of toric sublattices. The effect of different boundary conditions is definitely very interesting, which will be studied separately.

B. Decomposition of Ising configurations and quantum operators

Next, for a given decomposition \mathcal{M} of the base manifold M^D , we can define the decomposition of Ising configurations and operators. Without special note, in this paper we only consider $\frac{1}{2}$ -spins as basic degrees of freedom, and the σ^z (Ising) basis is always assumed. Given a model defined on M^D and one of its decomposition \mathcal{M} , when there is an inclusion $I : M_i^{d_1} \hookrightarrow M_j^{d_2}$, we can define the restriction of an arbitrary Ising configuration:

$$[\rho^c]_{M_i^{d_1}}^{M_j^{d_2}}(c_{M_j^{d_2}}) = c_{M_i^{d_1}}. \quad (9)$$

It maps $c_{M_j^{d_2}}$ to $c_{M_i^{d_1}}$ by simply dropping all degrees of freedom out of $M_i^{d_1}$. Here, $c_{M_i^{d_1}}$ and $c_{M_j^{d_2}}$ are Ising configurations respectively defined on $M_i^{d_1}$ and $M_j^{d_2}$. In the notation ρ^c , the superscript c literally stands for “configuration”. Then, for a given Ising configuration c and manifold decomposition \mathcal{M} , we can define the decomposition of the Ising configuration c on \mathcal{M} as $\Omega_{\mathcal{M}}^c(c)$, by taking the set of all restrictions of c onto sublattices inside \mathcal{M} . That is to say, we have

$$\Omega_{\mathcal{M}}^c(c) \equiv \{c_{M^{d_1}}\} \cup \{c_{M^{d_2}}\} \cup \cdots \cup \{c_{M^{d_k}}\}, \quad (10)$$

where $c_{M^{d_i}}$ refers to the restriction of the Ising configuration c onto a d_i -dimensional sublattice M^{d_i} . According to the definition of \mathcal{M} , the original Ising configuration c can be reconstructed from one of its decomposition $\Omega_{\mathcal{M}}^c(c)$. A pictorial demonstration of the restriction of Ising configurations is given in Fig. 3.

Similarly, with a given model and a decomposition \mathcal{M} , for a class of specially interesting operators, which are composed of σ^x operators (called “ X -operator” for simplicity), we can also define their restriction and decomposition. When there is an inclusion $I : M_i^{d_1} \hookrightarrow M_j^{d_2}$, the restriction

$$[\rho^o]_{M_i^{d_1}}^{M_j^{d_2}}(o_{M_j^{d_2}}) = o_{M_i^{d_1}} \quad (11)$$

maps $o_{M_j^{d_2}}$ to $o_{M_i^{d_1}}$ by dropping all σ^x operators defined on γ_{d_s} ’s out of $M_i^{d_1}$. Here, $o_{M_j^{d_2}}$ and $o_{M_i^{d_1}}$ are respectively X -operators totally supported on $M_j^{d_2}$ and $M_i^{d_1}$. In the notation ρ^o , the superscript o literally stands for “operator”. Again, for a given X -operator o and manifold decomposition \mathcal{M} , we can define the decomposition of the X -operator o on \mathcal{M} as $\Omega_{\mathcal{M}}^o(o)$, by taking the set

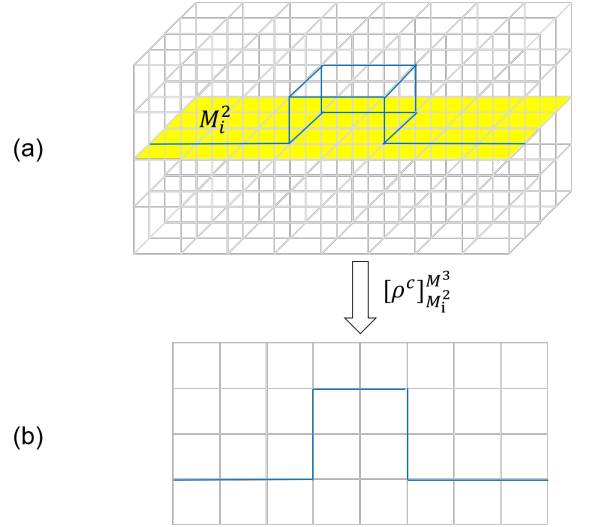


FIG. 3. **Restriction of Ising configurations in X-cube model.** Spins in X-cube model are located at centers of links. In (a), links with down spins are marked in blue. M_i^2 plane is highlighted in yellow. In (b), the restriction of the blue string composed of flipped spins onto subsystem M_i^2 is described. The restriction leads to a “humplike” shape Ising configuration.

of all restrictions of o onto sublattices inside \mathcal{M} . That is to say, we have

$$\Omega_{\mathcal{M}}^o(o) \equiv \{o_{M^{d_1}}\} \cup \{o_{M^{d_2}}\} \cup \cdots \cup \{o_{M^{d_k}}\}, \quad (12)$$

where $o_{M^{d_i}}$ refers to the restriction of the X -operator o onto a d_i -dimensional sublattice M^{d_i} . Since all σ^x operators commute with each other, an arbitrary X -operator o can also be reconstructed from one of its decomposition $\Omega_{\mathcal{M}}^o(o)$.

C. Subsystem ground state sector (SGS) as a holographic shadow of ground states

Then, we can define the decomposition of a ground state sector with a given manifold decomposition \mathcal{M} ⁵. Nevertheless, we have to at first consider how to define a ground state on a sublattice, as it is not as intuitive as the restriction of an Ising configuration. To solve this problem, we need to utilize the properties of ground states of $[d_n, d_s, d_l, D]$ models. For a ground state $|x\rangle$ of a $[d_n, d_s, d_l, D]$ model, it must satisfy the following conditions:

$$B_{\gamma_{d_n}}^l |x\rangle = |x\rangle, \forall l, \gamma_{d_n}; A_{\gamma_D} |x\rangle = |x\rangle, \forall \gamma_D. \quad (13)$$

⁵ We use “ground state sectors” instead of “ground states” in this section to emphasize that they can be regarded as sets of Ising configurations, as demonstrated in this subsection.

In σ^z basis, the constraints given by $B_{\gamma_{d_n}}^l$ terms can be realized by requiring all Ising configurations in $|x\rangle$ to satisfy certain conditions. As an example, in X-cube model denoted as $[0, 1, 2, 3]$, the constraints given by $B_{\gamma_0}^l$ terms require that a configuration c can only contain strings (formed by down spins) with trivalent vertices (see Sec. II B). The constraints given by A_{γ_D} terms require that, all Ising configurations, which can be transformed to each other by applying A_{γ_D} operators, must be equally superpositioned in a ground state $|x\rangle$. *Consequently, a ground state $|x\rangle$ of a $[d_n, d_s, d_l, D]$ model can be regarded as a set of Ising configuration c 's, and the set satisfies constraints given by both A and B terms.*

Similarly, we can define a *subsystem ground state sector* (SGS) on sublattice M^{d_i} , denoted as $x_{M^{d_i}}$. The SGS is a set of $c_{M^{d_i}}$'s. This set satisfies the following conditions:

- $c_{M^{d_i}}$ can be obtained as the restriction of a configuration c satisfying B constraints onto M^{d_i} . This condition results from the B constraints over original ground states.
- Two $c_{M^{d_i}}$'s belong to the same SGS, i.e., $x_{M^{d_i}}$, if and only if they can be connected under the action of $[\rho^o]_{M^{d_i}}^{M^D}(A_{\gamma_D})$. This condition results from the A constraints over original ground states. In other words, all elements in the SGS denoted as " $x_{M^{d_i}}$ " can be mapped to each other by $[\rho^o]_{M^{d_i}}^{M^D}(A_{\gamma_D})$.

Now we can see that, according to our definition of SGS, there is a well-defined restriction of a ground state x ⁶:

$$[\rho^x]_{M_i^{d_1}}^{M^D}(x) = x_{M_i^{d_1}} \quad (14)$$

which maps a ground state to an SGS on $M_i^{d_1}$ (to see the existence of this map, we only need to notice that by definition, the restriction of A_{γ_D} operators does not change any subsystem ground state sectors). Then we can define the decomposition of a ground state x on \mathcal{M} following exactly the same manner as Ising configurations and X -operators, by taking the set of all restrictions of x onto sublattices inside \mathcal{M} . So we have

$$\Omega_{\mathcal{M}}^x(x) \equiv \{x_{M^{d_1}}\} \cup \{x_{M^{d_2}}\} \cup \cdots \cup \{x_{M^{d_k}}\}, \quad (15)$$

where $x_{M^{d_i}}$ refers to the restriction of the ground state x on a d_i -dimensional sublattice M^{d_i} . *Intuitively, SGS can be regarded as a shadow of original ground states.* $\{x_{M^{d_i}}\}$ is the shadow.

Finally, we indicate that a ground state x of a $[d_n, d_s, d_l, D]$ model can be completely reconstructed from a decomposition of x on \mathcal{M} , as long as (a) \mathcal{M} contains $(d_s + 1)$ -dimensional subsystems, (b) $d_s - d_n = 1$

and (c) the base manifold M is a torus (a proof and some discussion about the cases when M has more complicated topology are given in Appendix B). For this reason, SGS can be regarded as a *holographic shadow* of original ground states.

In this paper, we only consider $[d_n, d_s, d_l, D]$ models defined on toric base manifolds with $d_s - d_n = 1$, and we always assume that our manifold decompositions contain $(d_s + 1)$ -dimensional subsystems. Thereupon, we can reconstruct ground states from SGS's. Nevertheless, not all combinations correspond to original ground states. In fact, a combination of SGS's has to satisfy certain *consistent conditions* to be corresponding to an original ground state. Obviously, all such consistent combinations are decompositions of original ground states, so we can use this property as a formal definition of the consistent conditions. More concrete description of consistent conditions depend on concrete models. In Sec. III D, we give a concrete example of consistent conditions in X-cube model.

In summary, once we have found the SGS's of a manifold decomposition \mathcal{M} and their consistent conditions, the ground state degeneracy can be obtained by counting the number of consistent combinations of SGS's. Nevertheless, it seems that there is no general method to derive the consistent conditions systematically.

D. Application in $[0, 1, 2, 3]$ model (X-cube model)

As an example, let us consider the ordinary (2)-decomposition (i.e. 2-dimensional foliation) of X-cube model on a 3-torus [18]. As we have reviewed in Sec. II B, the B constraints of Ising configurations require that all configuration c 's can only have trivalent vertices. On 2-dimensional subsystems, this constraint requires a $c_{M^2} = [\rho^c]_{M^2}^{M^3}(c)$ in an SGS to be a closed string configuration. And the restriction of A_{γ_3} stabilizers on 2-dimensional subsystems are just plaquette operators

$$A_{\gamma_2} \equiv [\rho^o]_{M_i^2}^{M^3}(A_{\gamma_3}) = \sigma_{\gamma_1^1}^x \sigma_{\gamma_1^2}^x \sigma_{\gamma_1^3}^x \sigma_{\gamma_1^4}^x, \quad (16)$$

where $\gamma_1^1, \gamma_1^2, \gamma_1^3, \gamma_1^4$ are four links of a plaquette γ_2 .

Therefore, an X-cube ground state can be determined by a consistent combination of 2D SGS's, and here an SGS can be identified as a 2D toric code ground state. Fig. 4 demonstrates such a restriction of a ground state. Then, we can see that the consistent condition is simply resulted from the fact that a logical operator $W(S^1) = \prod_{\gamma_1 \in S^1} \sigma_{\gamma_1}^x$ in X-cube model simultaneously change the SGS's on 2 intersecting M^2 's. In consequence, we can obtain all consistent combinations of SGS's by acting $W(S^1)$ operators on two intersecting M^2 's simultaneously from the combination where all SGS's have no non-local strings.

In general, we develop a method to represent all such consistent combinations with coloring patterns of certain graphs. In Sec. IV B, we demonstrate this coloring

⁶ To stress that x is a set of Ising configurations here, we omit the bracket notation.

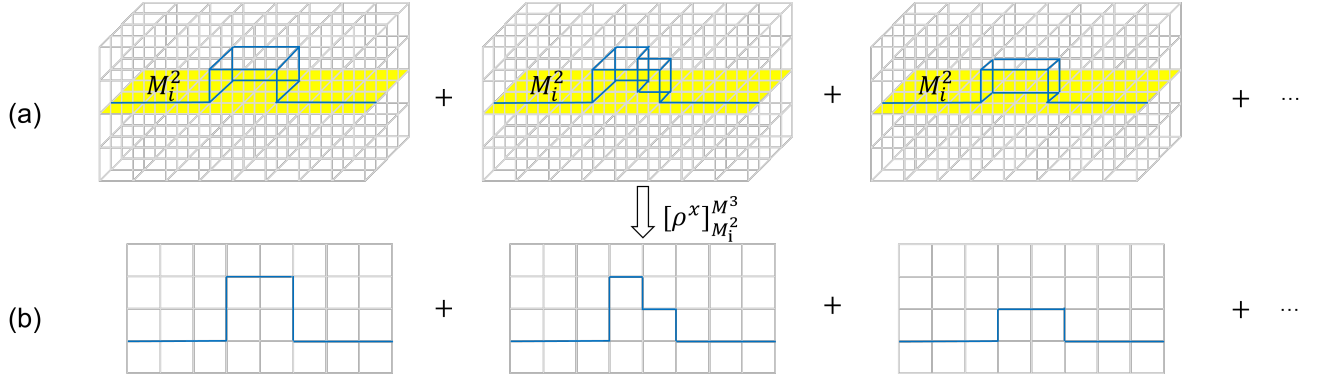


FIG. 4. **Restriction of a ground state in X-cube model.** The notation in this figure is the same as in Fig. 3. As we can see, the restriction of the ground state of X-cube model in (a) is equivalent to a ground state of a 2D toric code model.

method in detail, and give a concrete calculation of the GSD of X-cube model.

IV. GENERAL PROCEDURES AND COLORING METHOD

A. General procedures

Below we give a brief introduction of the key steps of the calculation. For $[0, 1, 2, D]$ and $[D - 3, D - 2, D - 1, D]$ models, similar to X-cube model (see Sec. III D), their SGS's on M^{d_s+1} 's can be identified as ground state sectors of some pure topological orders. That is to say, these SGS's can be obtained by exactly the same manner as ground states of some pure topological orders. As a result, in general, we can obtain the GSD of these models by the following steps:

- First, determine all SGS's on $(d_s + 1)$ -dimensional subsystems $x_{M_i^{d_s+1}} = [\rho^x]_{M_i^{d_s+1}}^{M^D}$ according to the definition of SGS given in Sec. III C.
- Second, find the consistent conditions between SGS's $x_{M_i^{d_s+1}}$'s.
- Third, calculate the number of consistent combinations of SGS's with a combinatorial method.

Here the counting of consistent combinations is not completely intuitive, since it involves the counting of high-dimensional objects. To avoid direct discussion about high dimensional geometric objects, it is convenient to use a combinatorial method, which converts the calculation to a coloring problem. In the rest part of this subsection, we will briefly demonstrate the construction of such coloring problems, and how to obtain GSD from them.

B. Coloring method: general description and application in $[0, 1, 2, 3]$ model (i.e., X-cube model)

In $[D - 3, D - 2, D - 1, D]$ and $[0, 1, 2, D]$ models with σ^z basis, logical operators are all generated by $W(S^{d_s}) = \prod_{\gamma \in S^{d_s}} \sigma_{\gamma}^x$ operators, where S^{d_s} is closed. Therefore, the SGS's on M^{d_s+1} 's are also distinguished by the action of $W(S^{d_s})$ operators (see Sec. V A and Sec. V C for a more detailed demonstration). So the consistent condition of these SGS's is simply resulted from the geometric fact that an S^{d_s} is always the intersection of $(D - d_s)$ M^{d_s+1} 's. Furthermore, as there are $\binom{D}{d_s}$ possible directions of S^{d_s} , and $W(S^{d_s})$ operators with S^{d_s} 's along different directions are independent, we can separate all ground states and SGS's into $\binom{D}{d_s}$ parts according to the direction of S^{d_s} . In general, the consistent condition of $x_{M_i^{d_s+1}}$'s in $[D - 3, D - 2, D - 1, D]$ and $[0, 1, 2, D]$ models is that we can only change SGS's of the same part on $(D - d_s)$ intersecting M^{d_s+1} 's simultaneously.

Therefore, we can use a coloring problem to visualize the consistent combinations of SGS's. We can construct a *characteristic graph* of a $[D - 3, D - 2, D - 1, D]$ or $[0, 1, 2, D]$ model for a given part of ground states. The construction is composed of the following steps:

- First, in a characteristic graph, we use a vertex to refer to an S^{d_s} belonging to the given part (i.e. along certain direction), and a straight line composed of edges to refer to an M^{d_s+1} .
- Second, lines intersecting at a vertex means that the corresponding M^{d_s+1} 's intersect at the S^{d_s} represented by the vertex.
- Then, we use colors of a line to refer to SGS's on the M^{d_s+1} . Because we only consider \mathbb{Z}_2 degrees of freedom in this paper, there are only 2 colors of lines. So we can simply label lines as "colored" and "uncolored".⁷

⁷ As all edges along the same line are always colored simultane-

- Finally, we require that all coloring operations should be done for a group of lines intersecting at one vertex simultaneously. Besides, we only consider coloring patterns that can be obtained by coloring the completely uncolored pattern.

In this manner, we can use a coloring pattern to represent a consistent combination of SGS's, and the computation of GSD is just equivalent to counting such coloring patterns.

As an example, we consider X-cube model. A brief introduction of the ground states of X-cube model is given in Sec. II B. In X-cube model, we have logical operators generated by $W(S^1) = \prod_{\gamma_{ds} \in S^1} \sigma_{\gamma_{ds}}^x$ operators. Thereupon, SGS's on M^2 's can also be changed by $W(S^1)$ operators. Obviously, $W(S^1)$ with S^1 along different directions are independent, so we can consider logical operators along the three spatial directions separately to obtain the GSD. Without loss of generality, here we consider the part of S^1 's along \hat{x}_1 direction. After that, we can see the consistent condition is resulted from the fact that a non-local S^1 along \hat{x}_1 must be the intersection of two perpendicular M^2 's respectively of $\langle \hat{x}_1, \hat{x}_2 \rangle$ and $\langle \hat{x}_1, \hat{x}_3 \rangle$ directions. So the consistent condition between x_{M^2} 's is that we can only change the SGS's on such two perpendicular M^2 's simultaneously. Due to that, for a X-cube model of the size $L \times L \times L$ with periodic boundary condition (PBC), the characteristic graph of the above mentioned part is just a square lattice of the size $L \times L$ with PBC. An example of the characteristic graph of X-cube model and its correspondence with ground states is given in Fig. 5.

Furthermore, in order to count the number of possible edge coloring patterns, we introduce a “characteristic group” based on following rules:

- An edge-coloring pattern of a characteristic graph is recognized as a group element.
- A vertex in the characteristic graph corresponds to a generator of the group, which is the edge-coloring pattern obtained by coloring all lines that intersect at the vertex. Different vertices correspond to different generators.
- The multiplication result of two elements is the pattern generated by the product of the corresponding $W(S^{d_s})$ operators. We can see the multiplication is equivalent to \mathbb{Z}_2 addition of coloring of lines. Fig. 6 gives an example of such a multiplication in X-cube model.
- Every generator defined above is its own inverse element.

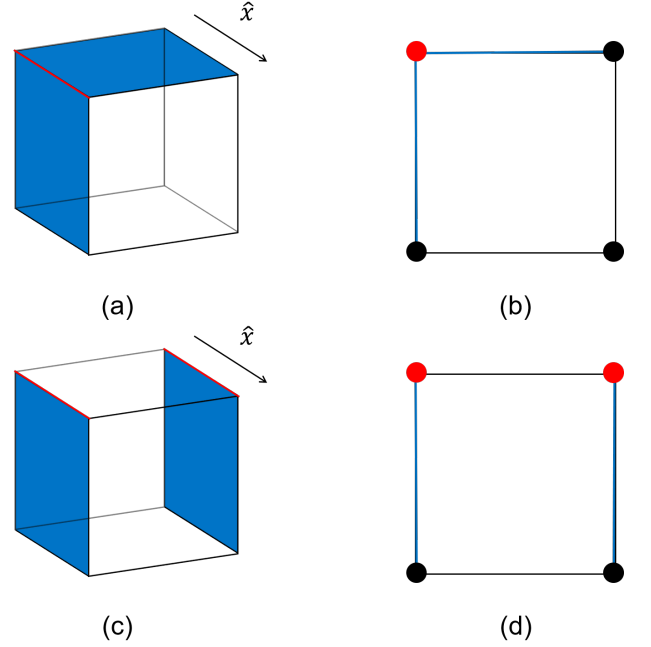


FIG. 5. **An example of the correspondence between an Ising configuration with non-contractible loops in X-cube model and the associated characteristic graph.** The red bar in (a) refers to the action of a $W(S^1)$ operator, where S^1 is a non-contractible loop, and the leaves M^2 with odd number of $W(S^1)$ actions are highlighted with blue. In (b), the vertex corresponding to the M^1 with a $W(S^1)$ action is colored with red, and its associated lines are colored with blue. In (c), we add another non-contractible loop that is parallel to the first one. Then, since the top leaf has been acted twice, it restores to the uncolored state, and in its corresponding coloring pattern of characteristic map (d), the line represents the top leaf is also uncolored.

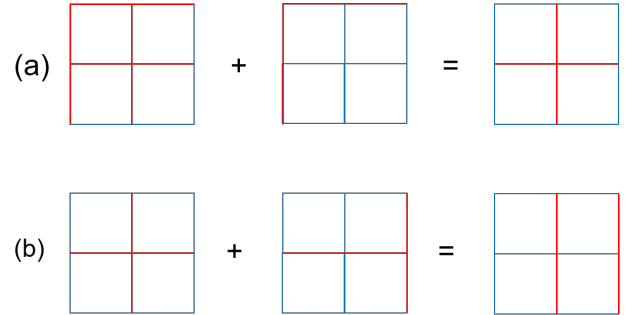


FIG. 6. **Examples of the multiplication of edge-coloring patterns.** Here we only draw the graph of the size 3×3 .

- The completely uncolored pattern is the identity element.

As the identity elements and inverse elements are already given in the above rules, we only need to check whether the above defined structure is closed and associative. According to our definition of the multiplication,

ously, in this paper we can use “edge” and “line” interchangeably. This is different from the usual case of mathematical discussion about graphs.

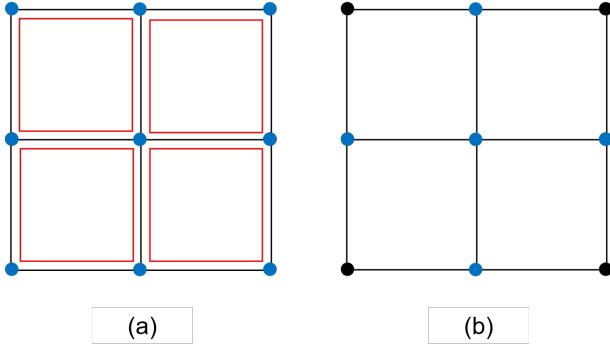


FIG. 7. **Pictorial demonstration of the elimination of additional degrees of freedom in the characteristic graphs.** The red squares in (a) represent the independent constraints associated with plaquettes, and the blue vertices represent the generators. In (b), since each independent constraint makes one generator in a plaquette redundant, we can simultaneously forget the redundant generators and the constraints to get 5 independent degrees of freedom.

all multiplication results can be generated by vertex generators, so the structure is closed. And since the multiplication is equivalent to the \mathbb{Z}_2 addition of coloring of lines, the multiplication is associative and commutative. Therefore, we can see that the structure is an Abelian group.

For an n -dimensional characteristic graph, the product of the vertex generators which form an n -cube equals to the identity. That is to say, not all vertex generators are independent. We need to find the number of independent generators to obtain the order of the characteristic group.

In the X-cube case, we continue with the discussion of characteristic graph of the \hat{x}_1 part, which is a square lattice of the size $L \times L$ with PBC. If we ignore the constraints given by 2-cubes in the graph, the characteristic group has L^2 vertex generators, so it should be a direct product of L^2 \mathbb{Z}_2 groups. When constraints are taken into consideration, we notice that only $(L-1)^2$ constraints that correspond to the γ_2 's (i.e. plaquettes)⁸ in the characteristic graph are necessary to generate all constraints. We can use each independent constraint to eliminate one generator in a plaquette. At last, only $L^2 - (L-1)^2 = 2L - 1$ independent \mathbb{Z}_2 degrees of freedom remain, so the group has 2^{2L-1} elements in total (Fig. 7 gives a pictorial demonstration of the elimination of degrees of freedom). Therefore, the ground state degeneracy of a X-cube model defined on a lattice of the size $L \times L \times L$ with PBC should be $(2^{2L-1})^3 = 2^{6L-3}$ (since we have dismantled the ground states into 3 independent parts), that is to say, we have $\log_2 GSD = 6L - 3$, which is consistent with the known result [18].

⁸ Apparently, there are L^2 γ_2 's in the characteristic graph, but we can verify that the extra γ_2 's resulted from the PBC can always be generated only by the γ_2 's that exist with OBC. It is a general rule due to the correspondence between vertices and generators.

In conclusion, once we have determined the SGS's and consistent conditions of a $[D-3, D-2, D-1, D]$ or $[0, 1, 2, D]$ model, we can then write down a series of characteristic graphs corresponding to ground states of different parts, and obtain the GSD by computing the orders of characteristic groups.

V. TYPICAL EXAMPLES

A. GSD of $[0, 1, 2, D]$ models on isotropic lattices

We begin with the discussion about $[0, 1, 2, D]$ models of the size $\underbrace{L \times L \times \dots \times L}_{D \text{ times}}$ with PBC.

- First, we analyze the ground states of a $[0, 1, 2, D]$ model to identity the SGS's. As a stabilizer code model, a ground state $|\phi\rangle$ of a $[0, 1, 2, D]$ model has to satisfy the following conditions:

$$\begin{aligned} B_{\gamma_0}^l |\phi\rangle &= |\phi\rangle, \quad \forall \gamma_0, l; \\ A_{\gamma_D} |\phi\rangle &= |\phi\rangle, \quad \forall \gamma_D. \end{aligned}$$

In σ^z basis, conditions given by B terms require in ground states, all Ising configurations c can only have S^1 (i.e. straight strings) and vertices emanating D perpendicular S^1 's. And conditions given by A terms require all Ising configuration c 's that can be connected by action of A terms to belong to the same ground state.

For SGS's on M^2 , we can see that subsystem Ising configurations c_{M^2} 's can only have S^1 and vertices emanating 2 perpendicular S^1 's, that is to say, $[\rho^c]_{M^2}^{M^D}(c) = c_{M^2}$ can only have closed loops. And an SGS is composed of all such c_{M^2} 's that can be connected by $[\rho^o]_{M^2}^{M^D}(A_{\gamma_D}) = A_{\gamma_2} = \prod_{\gamma_1 \in \gamma_2} \sigma_{\gamma_1}^x$ operators. In summary, an SGS on an M^2 is equivalent to a ground state of a 2D toric code model. Different SGS's can be distinguished by the action of non-local $W(S^1) = \prod_{\gamma_1 \in S^1} \sigma_{\gamma_1}^x$ operators.

- Second, we consider the consistent conditions between these SGS's. Since $W(S^1)$'s with S^1 along different directions contribute to SGS's independently, without loss of generality, now we restrict our discussion to S^1 's along \hat{x}_1 direction. As discussed in Sec. IV, the consistent conditions requires a $W(S^1)$ operator to simultaneously act on $(D-1)$ intersecting M^2 's. For S^1 's along \hat{x}_1 direction, the $(D-1)$ M^2 's must be respectively of the $\langle \hat{x}_1, \hat{x}_2 \rangle$, $\langle \hat{x}_1, \hat{x}_3 \rangle$, $\langle \hat{x}_1, \hat{x}_4 \rangle$, \dots , and $\langle \hat{x}_1, \hat{x}_D \rangle$ directions.
- Third, we summarize the above data of SGS's and their consistent conditions in the characteristic graph, and obtain the GSD from the graph. For the part with S^1 's along \hat{x}_1 direction, the characteristic graph is a $(D-1)$ -dimensional hypercubic

lattice with PBC. So according to our discussion in Sec. IV, the characteristic group has $L^{(D-1)}$ generators (corresponding to the vertices in the graph) and $(L-1)^{(D-1)}$ constraints (corresponding to the $(D-1)$ -cubes in the graph). Because the system we are considering is isomorphic, all the D parts give the same results, and the final GSD is just given by the product of the results of different parts.

Finally, we obtain that the GSD of $[0, 1, 2, D]$ models is given by:

$$\begin{aligned} \log_2 \text{GSD} &= D \times (L^{D-1} - (L-1)^{D-1}) \\ &= D \times \sum_{n=0}^{D-2} \binom{D-1}{n} (-1)^{D+n} L^n. \end{aligned} \quad (17)$$

When $D = 3$, the result automatically restores to the X-cube case.

B. GSD of $[0, 1, 2, D]$ models on anisotropic lattices

For a $[0, 1, 2, D]$ model defined on a lattice of the size $\underbrace{L_1 \times L_2 \times L_3 \times \cdots \times L_D}_{D \text{ times}}$ with PBC, a ground state follows exactly the same manner as in the isotropic case. That is to say, the SGS's are also equivalent to 2D toric code ground states. Besides, the consistent conditions are also the same. The anisotropic condition only influence the sizes of characteristic graphs.

For the part of S^1 's along \hat{x}_i ($1 \leq i \leq D$) direction, the characteristic graph is a $(D-1)$ -dimensional hypercubic lattice of the size $L_1 \times L_2 \times L_3 \times \cdots \times \hat{L}_i \times \cdots \times L_D$. Here \hat{L}_i means that L_i is not included in the product. Therefore, the corresponding characteristic group has $L_1 \times L_2 \times L_3 \times \cdots \times \hat{L}_i \times \cdots \times L_D$ generators and $(L_1 - 1) \times (L_2 - 1) \times (L_3 - 1) \times \cdots \times (\hat{L}_i - 1) \times \cdots \times (L_D - 1)$ independent constraints.

As the contribution of other parts can be similarly obtained, the GSD of a $[0, 1, 2, D]$ model defined on a

anisotropic lattice is given by:

$$\begin{aligned} \log_2 \text{GSD} &= \sum_j^D \left\{ \left(\frac{1}{L_j} \prod_i^D L_i \right) - \left(\frac{1}{L_j - 1} \prod_i^D (L_i - 1) \right) \right\} \\ &= 2 \times \left(\sum_{k_1}^D \sum_{k_2}^{k_1-1} \frac{1}{L_{k_1} L_{k_2}} \prod_n L_n \right) \\ &\quad - 3 \times \left(\sum_{k_1}^D \sum_{k_2}^{k_1-1} \sum_{k_3}^{k_2-1} \frac{1}{L_{k_1} L_{k_2} L_{k_3}} \prod_n L_n \right) \\ &\quad + 4 \times \left(\sum_{k_1}^D \sum_{k_2}^{k_1-1} \sum_{k_3}^{k_2-1} \sum_{k_4}^{k_3-1} \frac{1}{L_{k_1} L_{k_2} L_{k_3} L_{k_4}} \prod_n L_n \right) \\ &\quad - \dots \\ &\quad + (-1)^{D-1} (D-1) \sum_n^D L_n \\ &\quad + (-1)^D D. \end{aligned}$$

C. GSD of $[D-3, D-2, D-1, D]$ models on isotropic lattices

Then we consider $[D-3, D-2, D-1, D]$ models of the size $\underbrace{L \times L \times \cdots \times L}_{D \text{ times}}$ with PBC.

- First, we analyze the ground states of a $[D-3, D-2, D-1, D]$ model to identify the SGS's. As a $[D-3, D-2, D-1, D]$ model is also a stabilizer code, a ground state $|\phi\rangle$ of a $[D-3, D-2, D-1, D]$ model analogously satisfy the following conditions:

$$\begin{aligned} B_{\gamma_{D-3}}^l |\phi\rangle &= |\phi\rangle, \quad \forall \gamma_{D-3}, l; \\ A_{\gamma_D} |\phi\rangle &= |\phi\rangle, \quad \forall \gamma_D. \end{aligned}$$

Here we should notice that the definition of A_{γ_D} terms are different from the A terms in a $[0, 1, 2, D]$ models, though they share the same form (see Sec. II B). In σ^z basis, conditions given by B terms require that in ground states, all Ising configuration c 's can only have S^{D-2} 's and S^{D-3} 's emanating 3 perpendicular S^{D-2} 's. And conditions given by A terms require all c 's that can be connected by action of A terms to belong to the same ground state.

For SGS's on M^{D-1} , we can see that subsystem Ising configurations $c_{M^{D-1}}$'s can only have S^{D-2} 's and S^{D-3} 's emanating 2 perpendicular S^{D-2} 's, that is to say, $[\rho^c]_{M^{D-1}}^D(c) = c_{M^{D-1}}$ can only have closed $(D-2)$ -dimensional objects. And an SGS is composed of all such $c_{M^{D-1}}$'s that can be connected by $[\rho^0]_{M^{D-1}}^D(A_{\gamma_D}) = A_{\gamma_{D-1}}$ operators. Different SGS's can be distinguished by the action of non-local $W(S^{D-2}) = \prod_{\gamma_{D-2} \in S^{D-2}} \sigma_{\gamma_{D-2}}^x$ operators, where S^{D-2} is closed.

- Second, we consider the consistent conditions between these SGS's on M^{D-1} 's. Again, $W(S^{D-2})$'s with S^{D-2} along different directions contribute to SGS's independently. Without loss of generality, we restrict our discussion to S^{D-2} 's along $\langle \hat{x}_1, \hat{x}_2, \hat{x}_3, \dots, \hat{x}_{D-2} \rangle$ direction. As discussed in Sec. IV, the consistent condition requires a $W(S^{D-2})$ operator to simultaneously act on 2 intersecting M^{D-1} 's. For S^{D-2} 's along $\langle \hat{x}_1, \hat{x}_2, \hat{x}_3, \dots, \hat{x}_{D-2} \rangle$ direction, the 2 M^{D-1} 's must be respectively of the $\langle \hat{x}_1, \hat{x}_2, \hat{x}_3, \dots, \hat{x}_{D-2}, \hat{x}_{D-1} \rangle$ and $\langle \hat{x}_1, \hat{x}_2, \hat{x}_3, \dots, \hat{x}_{D-2}, \hat{x}_D \rangle$ directions.
- Third, we summarize the above data of SGS's and their consistent conditions in the characteristic graph, and obtain the GSD from the graph. For the part with S^{D-2} 's along $\langle \hat{x}_1, \hat{x}_2, \hat{x}_3, \dots, \hat{x}_{D-2} \rangle$ direction, the characteristic graph is a 2-dimensional square lattice with PBC. So according to our discussion in Sec. IV, the characteristic group has L^2 generators (corresponding to the vertices in the graph) and $(L-1)^2$ constraints (corresponding to the 2-cubes in the graph). Because the system we are considering is isomorphic, all the $\binom{D}{D-2}$ parts give the same results, and the final GSD is just given by the product of the results of different parts.

Finally, we obtain that the GSD of $[D-3, D-2, D-1, D]$ models is given by:

$$\begin{aligned} \log_2 GSD &= \binom{D}{D-2} \times (L^2 - (L-1)^2) \\ &= \binom{D}{D-2} \times (2L-1) \end{aligned} \quad (18)$$

$$= (D^2 - D) \times L - \frac{D^2 - D}{2}. \quad (19)$$

Again, when $D=3$, the result will restore to the X-cube case.

D. GSD of $[D-3, D-2, D-1, D]$ models on anisotropic lattices

The difference between a $[D-3, D-2, D-1, D]$ model defined on a lattice of the size $\underbrace{L_1 \times L_2 \times L_3 \times \dots \times L_D}_{D \text{ times}}$ and the isotropic case is similar to a $[0, 1, 2, D]$ model. All SGS's and their consistent conditions stay the same, we only need to consider variance of the characteristic graphs.

For the part of S^{D-2} 's along $\langle \hat{x}_1, \hat{x}_2, \hat{x}_3, \dots, \hat{x}_{D-2} \rangle$ direction, the characteristic graph is a 2-dimensional square lattice with the size $L_{D-1} \times L_D$. Therefore, the corresponding characteristic group has $L_{D-1} \times L_D$ generators and $(L_{D-1} - 1) \times (L_D - 1)$ independent constraints.

As the contribution of other parts can be similarly obtained, the GSD of a $[D-3, D-2, D-1, D]$ model defined on an anisotropic lattice is given by:

$$\begin{aligned} \log_2 GSD &= \sum_i^D \sum_j^{i-1} \{L_i \times L_j - (L_i - 1) \times (L_j - 1)\} \\ &= \sum_i^D \sum_j^{i-1} \{L_i + L_j - 1\} \\ &= \sum_i^D (D-1) \times L_i - \frac{D^2 - D}{2}. \end{aligned}$$

VI. DISCUSSIONS AND CONCLUSIONS

By comparing the GSD of X-cube, $[0, 1, 2, D]$ and $[D-3, D-2, D-1, D]$ models summarized in Table I, we have the following observations. First, in a $[0, 1, 2, D]$ model, the $\log_2 GSD$ becomes a polynomial. Such a polynomial contains not only the linear and constant terms, but also terms of any degrees that are smaller than $D-1$. Besides, in a $[D-3, D-2, D-1, D]$ model, the $\log_2 GSD$ is of same form as X-cube model.

The polynomials $\log_2 GSD$ in $[0, 1, 2, D]$ models are the most interesting and unprecedented result here, while a complete understanding of these polynomials is still lacking. Here we believe it is beneficial to give some primary discussions about the relation between polynomials $\log_2 GSD$ and other features of fracton orders.

First, as we have mentioned in Sec. I, in $[0, 1, 2, D]$ models, from the perspective of foliated fracton orders, their leaves admit foliation structures as well. Therefore, we may recognize the orders in $[0, 1, 2, D]$ models as multi-level foliated fracton orders. Or from the perspective of decomposition, it means that when the whole system is in a ground state, the SGS in a $(D-1)$ -dimensional subsystem also looks like a ground state of a fracton model (more exactly, it looks like a ground state of a $[0, 1, 2, D-1]$ model). Mathematically, we have already known the relation between the coefficients in the $\log_2 GSD$ of X-cube model and the 2-foliation of the manifold where the system is defined [18]. The coefficients in all polynomials found in this work are expected to reflect a series of topological and geometric properties of the quantum models and background lattice. For example, as the multi-level foliation structure suggests, the coefficients are likely to contain information of subsystems of various dimensions. Now, as a rigorous and complete discussion of multi-level foliation is still under exploration, some future works seem to be necessary to clarify the relationship between models like $[1, 2, 3, D]$ and multi-level foliation structures.

Second, in our previous work, topological excitations are classified into *trivial excitations* (denoted as \mathbb{I}), *simple excitations* (denoted as \mathbb{E}^s), *complex excitations* (denoted as \mathbb{E}^c) and *intrinsically disconnected excitations*

(denoted as E^d) in $[d_n, d_s, d_l, D]$ models [50], according to mobility and deformability of topological excitations. Fracton physics of spatially extended excitations can exist in all nontrivial excitations, i.e., E^s , E^c and E^d , as studied in Ref. [50]. While the GSD polynomials are also derived from $[d_n, d_s, d_l, D]$ models, one may wonder what is the relation between GSD polynomials and existence of nontrivial excitations. A similar question can be answered in (2+1) Abelian topological order where GSD on a torus is equal to the number of distinct topological excitations. But it is hard to firmly answer the question in the present fracton models, which is left to future work.

Besides, we believe the mathematical aspect of polynomial $\log_2 GSD$ may be particularly interesting. Inspired from the foliated fracton orders, we believe the coefficients of such polynomials may reflect the properties of various subsystems. While if we consider such a polynomial as a whole, the polynomial itself may represent a novel characteristic of topology and geometry of a high-dimensional object. That is to say, how these coefficients interact each other, and how these information of different subsystems are integrated into a whole, may require more mathematical exploitation. These questions may be answered by considering $[d_n, d_s, d_l, D]$ models on general manifolds [18] which are beyond toric manifolds used in this work.

From another perspective, we can see that the relation between $[0, 1, 2, 4]$ and X-cube model is similar to the relation between X-cube and 2D toric code model. It makes $[0, 1, 2, 4]$ model kind of a “fracton order of fracton order”. Such an observation makes us believe that better knowledge about the relation between higher-dimensional fracton orders and 3D fracton orders may be beneficial to gain deeper insights about a general theory of fracton orders and especially the physics of non-manifold excitations found in Ref. [50].

In this paper, as we have restricted our discussion to models with $[d_n, d_s, d_l, D]$ models with $d_s - d_n = 1$, the generality of computing GSD based on SGS’s is still kind of vague. If it is possible to generalize our computation to other foliated fracton orders, or even Type-II fracton orders, like Haah’s code, is quite worth exploring. Nonetheless, until now we can only case-by-case check if the SGS method works for a given model. Besides, as in principle, we need to exhaust all manifold decomposition \mathcal{M} to assert the SGS method does not work for a model, it seems difficult to understand when the SGS method would fail.

In order to compute the GSD, we demonstrate a method to represent a ground state with a collection of lower-dimensional data. Then it is a natural question to ask if such lower-dimensional representations can be applied to excited states. Since excitations can have representations as composites of collections of subsystem superselection sectors with the form of $(e\ m) + (m\ e)$, such composites may be recognized as being composed of “entangled” topological excitations. Therefore, we believe the decomposition of excitations may also reveal some

interesting features of fracton orders, which will be presented in [87].

ACKNOWLEDGEMENTS

This work was supported in part by the Sun Yat-sen University startup grant, Guangdong Basic and Applied Basic Research Foundation under Grant No. 2020B1515120100, National Natural Science Foundation of China (NSFC) Grant (No. 11847608 & No. 12074438).

Appendix A: Notations and conventions

- γ_d : d-cube. Firstly appears in Sec. II A.
- S^d : a d -dimensional analog of a cuboid. Firstly appears in Sec. II A.
- M^d : a d -dimensional manifold. Firstly appears in Sec. III.
- \mathcal{M} : a (d_1, d_2, \dots, d_k) -decomposition of a given D -dimensional base manifold M^D . Firstly appears in Sec. III.
- $[\rho^c]_{M_i^{d_1}}^{M_j^{d_2}}(c_{M_j^{d_2}})$: a restriction of an Ising configuration on $M_j^{d_2}$ to one of its subsystem $M_i^{d_1}$. Firstly appears in Sec. III.
- $\Omega_{\mathcal{M}}^c(c)$: a decomposition of an Ising configuration c on the base manifold to a collection of subsystem specified by \mathcal{M} . Firstly appears in Sec. III.
- $[\rho^o]_{M_i^{d_1}}^{M_j^{d_2}}(o_{M_j^{d_2}})$: a restriction of an X-operator on $M_j^{d_2}$ to one of its subsystem $M_i^{d_1}$. Firstly appears in Sec. III.
- $\Omega_{\mathcal{M}}^o(o)$: a decomposition of an X-operator o on the base manifold to a collection of subsystem specified by \mathcal{M} . Firstly appears in Sec. III.
- c_M : an Ising configuration c on manifold M . When the manifold can be specified from the context, we may omit the subscript M .
- $[\rho^x]_{M_i^{d_1}}^{M^D}(x)$: a restriction of a ground state x on the base manifold M^D to one of its subsystem $M_i^{d_1}$. Firstly appears in Sec. III.
- $\Omega_{\mathcal{M}}^o(o)$: a decomposition of an a ground state x on the base manifold to a collection of subsystem specified by \mathcal{M} . Firstly appears in Sec. III.
- GSD: ground state degeneracy. Firstly appears in Sec. I.
- SGS: subsystem ground state sector. Firstly appears in Sec. III.

- PBC: periodic boundary condition. Firstly appears in Sec. IV.
- OBC: open boundary condition. Firstly appears in Sec. IV.

Appendix B: Proof of the isomorphism between ground states and consistent combinations of SGS's

In this Appendix, we prove that for a $[d_n, d_s, d_l, D]$ model defined on toric M with a manifold decomposition \mathcal{M} , given that (a) \mathcal{M} contains $(d_s + 1)$ -dimensional subsystems and (b) $d_s - d_n = 1$, then there is always an isomorphism between ground states of a $[d_n, d_s, d_l, D]$ model and consistent combinations of SGS's on \mathcal{M} . That is to say, if a combination of SGS's can be obtained as a decomposition of a ground state x on \mathcal{M} , then we can always obtain the original ground state x merely from the information of these SGS's.

Proof. We use contradiction to prove it. For a given \mathcal{M} including $\{M^{d_s+1}\}$, we assume that there exists a pair of ground states $x_1 \neq x_2$, such that

$$\Omega_{\mathcal{M}}^x(x_1) = \Omega_{\mathcal{M}}^x(x_2). \quad (\text{B1})$$

As x_1 and x_2 are different ground states, they can always be connected by a logical operator denoted as o_x . So we have

$$o_x |x_1\rangle = |x_2\rangle. \quad (\text{B2})$$

In a $[d_n, d_s, d_l, D]$ model, when $d_s - d_n = 1$, we can consider a complete set of logical operators generated by $W(S^{d_s}) = \prod_{\gamma_{d_s} \in S^{d_s}} \sigma_{\gamma_{d_s}}^x$, where S^{d_s} is closed. These logical operators are composed of σ^x operators along closed S^{d_s} 's. Here, as an S^{d_s} is required to be totally flat, a closed S^{d_s} must be extended along all d_s directions to avoid any boundaries.

Then, we need to notice not all such $W(S^{d_s})$ generators are independent to each other. The product of 2^{D-d_s} $W(S^{d_s})$'s equals to the trivial logical operator,

when these S^{d_s} 's form the d_s -dimensional boundary of an S^D that is extended along d_s directions. That is to say, these S^{d_s} 's satisfy the following conditions:

- All S^{d_s} 's are parallel;
- There are only 2 or 0 S^{d_s} 's in an M^{d_s+1} .

Such a product is trivialized as it can be written as a product of A_{γ_D} operators.

As o_x preserves all SGS's, from Eq. B1, we can see that $\forall M^{d_s+1} \in \mathcal{M}$, $[\rho^o]_{M^{d_s+1}}^M(o_x)$ must be a product of parallel pairs of $W(S^{d_s})$ operators. Therefore, $\forall M^{d_s+2} \subset M$, $[\rho^o]_{M^{d_s+2}}^M(o_x)$ must be a product of parallel quadruples of $W(S^{d_s})$ operators. Iteratively, we obtain that o_x must be the product of groups of 2^{D-d_s} parallel $W(S^{d_s})$ operators. Consequently, on a toric base manifold M , by removing $W(S^{d_s})$ operators which compose trivial logical operators, o_x can be transformed to the identity operator, whose restrictions on all M^{d_s+1} 's are trivial. As a result, o_x has to be the trivial logical operator, and it is against our assumption that $x_1 \neq x_2$. \square

Thereupon, the map from ground states to combinations of subsystem ground state sectors is an injection. So a ground state x of a $[d_n, d_s, d_l, D]$ model can be reconstructed from its decomposition on \mathcal{M} .

Finally, we make some comments about the case when M is not a torus, but a manifold with more complicated topology. Then, the above proof may fail as even though $[\rho^o]_{M^{d_s+1}}^M(o_x)$ is a product of 2 $W(S^{d_s})$ operators for an arbitrary $M^{d_s+1} \in \mathcal{M}$, it may be impossible to find a product of A_{γ_D} operators to reduce all these $W(S^{d_s})$ operators simultaneously. In that case, to reconstruct the original ground state, except for SGS's, we may also need additional information depending on the topology of the base manifold M . Nevertheless, it is also possible that the original ground state can be reconstructed by adding new subsystems to manifold decomposition \mathcal{M} . As far as we know, more works are needed to obtain a systematic understanding of such problems.

-
- [1] Xiao-Gang Wen, "Colloquium: Zoo of quantum-topological phases of matter," *Rev. Mod. Phys.* **89**, 041004 (2017).
 - [2] X. G. Wen, "Vacuum degeneracy of chiral spin states in compactified space," *Phys. Rev. B* **40**, 7387–7390 (1989).
 - [3] Xiao-Gang Wen, "A theory of 2+1d bosonic topological orders," *Natl. Sci. Rev.* (2015), 10.1093/nsr/nwv077, arXiv:1506.05768.
 - [4] Rahul M. Nandkishore and Michael Hermele, "Fractons," *Annual Review of Condensed Matter Physics* **10**, 295–313 (2019), arXiv:1803.11196 [cond-mat.str-el].
 - [5] Michael Pretko, Xie Chen, and Yizhi You, "Fracton phases of matter," *International Journal of Modern Physics A* **35**, 2030003 (2020), arXiv:2001.01722 [cond-mat.str-el].
 - [6] Sagar Vijay, Jeongwan Haah, and Liang Fu, "A new kind of topological quantum order: A dimensional hierarchy of quasiparticles built from stationary excitations," *Phys. Rev. B* **92**, 235136 (2015).
 - [7] Sagar Vijay, Jeongwan Haah, and Liang Fu, "Fracton topological order, generalized lattice gauge theory, and duality," *Phys. Rev. B* **94**, 235157 (2016).
 - [8] Abhinav Prem, Jeongwan Haah, and Rahul Nandkishore, "Glassy quantum dynamics in translation invariant fracton models," *Physical Review B* (2017), 10.1103/PhysRevB.95.155133, arXiv:1702.02952.

- [9] Claudio Chamon, “Quantum glassiness in strongly correlated clean systems: An example of topological overprotection,” *Phys. Rev. Lett.* **94**, 040402 (2005).
- [10] Wilbur Shirley, Kevin Slagle, and Xie Chen, “Foliated fracton order from gauging subsystem symmetries,” *SciPost Phys.* **6**, 41 (2019).
- [11] Han Ma, Ethan Lake, Xie Chen, and Michael Hermele, “Fracton topological order via coupled layers,” *Phys. Rev. B* **95**, 245126 (2017).
- [12] Jeongwan Haah, “Local stabilizer codes in three dimensions without string logical operators,” *Phys. Rev. A* **83**, 042330 (2011).
- [13] Daniel Bulmash and Maissam Barkeshli, “Gauging fractons: Immobile non-Abelian quasiparticles, fractals, and position-dependent degeneracies,” *Phys. Rev. B* **100**, 155146 (2019), [arXiv:1905.05771 \[cond-mat.str-el\]](#).
- [14] Abhinav Prem and Dominic Williamson, “Gauging permutation symmetries as a route to non-Abelian fractons,” *SciPost Physics* **7**, 068 (2019), [arXiv:1905.06309 \[cond-mat.str-el\]](#).
- [15] Kevin Slagle and Yong Baek Kim, “Quantum field theory of X-cube fracton topological order and robust degeneracy from geometry,” *Physical Review B* **96** (2017), 10.1103/PhysRevB.96.195139.
- [16] Wilbur Shirley, Kevin Slagle, and Xie Chen, “Fractional excitations in foliated fracton phases,” *Annals of Physics* **410**, 167922 (2019), [arXiv:1806.08625 \[cond-mat.str-el\]](#).
- [17] Kevin Slagle, David Aasen, and Dominic Williamson, “Foliated field theory and string-membrane-net condensation picture of fracton order,” *SciPost Physics* **6**, 43 (2019).
- [18] Wilbur Shirley, Kevin Slagle, Zhenghan Wang, and Xie Chen, “Fracton models on general three-dimensional manifolds,” *Phys. Rev. X* **8**, 031051 (2018).
- [19] Abhinav Prem, Michael Pretko, and Rahul M. Nandkishore, “Emergent phases of fractonic matter,” *Phys. Rev. B* **97**, 085116 (2018), [arXiv:1709.09673 \[cond-mat.str-el\]](#).
- [20] Shriya Pai and Michael Pretko, “Dynamical Scar States in Driven Fracton Systems,” *Phys. Rev. Lett.* **123**, 136401 (2019), [arXiv:1903.06173 \[cond-mat.stat-mech\]](#).
- [21] Pablo Sala, Tibor Rakovszky, Ruben Verresen, Michael Knap, and Frank Pollmann, “Ergodicity Breaking Arising from Hilbert Space Fragmentation in Dipole-Conserving Hamiltonians,” *Physical Review X* **10**, 011047 (2020), [arXiv:1904.04266 \[cond-mat.str-el\]](#).
- [22] Michael Pretko and Leo Radzihovsky, “Fracton-Elasticity Duality,” *Phys. Rev. Lett.* **120**, 195301 (2018), [arXiv:1711.11044 \[cond-mat.str-el\]](#).
- [23] Michael Pretko, “Emergent gravity of fractons: Mach’s principle revisited,” *Physical Review D* (2017), 10.1103/PhysRevD.96.024051, [arXiv:1702.07613](#).
- [24] Han Ma, Michael Hermele, and Xie Chen, “Fracton topological order from the higgs and partial-confinement mechanisms of rank-two gauge theory,” *Phys. Rev. B* **98**, 035111 (2018).
- [25] Michael Pretko, “Generalized electromagnetism of subdimensional particles: A spin liquid story,” *Phys. Rev. B* **96**, 035119 (2017).
- [26] Leo Radzihovsky and Michael Hermele, “Fractons from Vector Gauge Theory,” *Phys. Rev. Lett.* **124**, 050402 (2020), [arXiv:1905.06951 \[cond-mat.str-el\]](#).
- [27] Arpit Dua, Isaac H. Kim, Meng Cheng, and Dominic J. Williamson, “Sorting topological stabilizer models in three dimensions,” *Phys. Rev. B* **100**, 155137 (2019), [arXiv:1908.08049 \[quant-ph\]](#).
- [28] Andrey Gromov, “Chiral topological elasticity and fracton order,” *Phys. Rev. Lett.* **122**, 076403 (2019).
- [29] Andrey Gromov, “Towards classification of fracton phases: The multipole algebra,” *Phys. Rev. X* **9**, 031035 (2019).
- [30] Vedika Khemani, Michael Hermele, and Rahul Nandkishore, “Localization from hilbert space shattering: From theory to physical realizations,” *Phys. Rev. B* **101**, 174204 (2020).
- [31] Michael Pretko and Rahul M. Nandkishore, “Localization of extended quantum objects,” *Phys. Rev. B* **98**, 134301 (2018).
- [32] Dominic J. Williamson, Zhen Bi, and Meng Cheng, “Fractonic matter in symmetry-enriched $u(1)$ gauge theory,” *Phys. Rev. B* **100**, 125150 (2019).
- [33] Arpit Dua, Dominic J. Williamson, Jeongwan Haah, and Meng Cheng, “Compactifying fracton stabilizer models,” *Phys. Rev. B* **99**, 245135 (2019).
- [34] Bowen Shi and Yuan-Ming Lu, “Deciphering the nonlocal entanglement entropy of fracton topological orders,” *Phys. Rev. B* **97**, 144106 (2018).
- [35] Hao Song, Abhinav Prem, Sheng-Jie Huang, and M. A. Martin-Delgado, “Twisted fracton models in three dimensions,” *Phys. Rev. B* **99**, 155118 (2019).
- [36] Han Ma and Michael Pretko, “Higher-rank deconfined quantum criticality at the lifshitz transition and the exciton bose condensate,” *Phys. Rev. B* **98**, 125105 (2018).
- [37] Kevin Slagle, “Foliated quantum field theory of fracton order,” *Phys. Rev. Lett.* **126**, 101603 (2021).
- [38] Dominic J. Williamson and Trithep Devakul, “Type-II fractons from coupled spin chains and layers,” *Phys. Rev. B* **103**, 155140 (2021), [arXiv:2007.07894 \[cond-mat.str-el\]](#).
- [39] Pranay Gorantla, Ho Tat Lam, Nathan Seiberg, and Shu-Heng Shao, “More exotic field theories in 3+1 dimensions,” *SciPost Physics* **9**, 073 (2020), [arXiv:2007.04904 \[cond-mat.str-el\]](#).
- [40] Dung Nguyen, Andrey Gromov, and Sergej Moroz, “Fracton-elasticity duality of two-dimensional superfluid vortex crystals: defect interactions and quantum melting,” *SciPost Physics* **9**, 076 (2020), [arXiv:2005.12317 \[cond-mat.quant-gas\]](#).
- [41] Michael Pretko, S. A. Parameswaran, and Michael Hermele, “Odd fracton theories, proximate orders, and parton constructions,” *Phys. Rev. B* **102**, 205106 (2020), [arXiv:2004.14393 \[cond-mat.str-el\]](#).
- [42] Dominic J. Williamson and Meng Cheng, “Designer non-Abelian fractons from topological layers,” *arXiv e-prints*, [arXiv:2004.07251 \(2020\)](#), [arXiv:2004.07251 \[cond-mat.str-el\]](#).
- [43] David T. Stephen, José Garre-Rubio, Arpit Dua, and Dominic J. Williamson, “Subsystem symmetry enriched topological order in three dimensions,” *Physical Review Research* **2**, 033331 (2020), [arXiv:2004.04181 \[cond-mat.str-el\]](#).
- [44] Nathan Seiberg and Shu-Heng Shao, “Exotic $U(1)$ Symmetries, Duality, and Fractons in 3+1-Dimensional Quantum Field Theory,” *SciPost Phys.* **9**, 46 (2020).
- [45] Andrey Gromov, Andrew Lucas, and Rahul M. Nandkishore, “Fracton hydrodynamics,” *Physical Review Research* **2**, 033124 (2020), [arXiv:2003.09429 \[cond-mat.str-el\]](#).

- [46] Wilbur Shirley, “Fractonic order and emergent fermionic gauge theory,” arXiv e-prints , arXiv:2002.12026 (2020), [arXiv:2002.12026 \[cond-mat.str-el\]](#).
- [47] David Aasen, Daniel Bulmash, Abhinav Prem, Kevin Slagle, and Dominic J. Williamson, “Topological defect networks for fractons of all types,” *Physical Review Research* **2**, 043165 (2020), [arXiv:2002.05166 \[cond-mat.str-el\]](#).
- [48] Xiao-Gang Wen, “Systematic construction of gapped nonliquid states,” *Physical Review Research* **2**, 033300 (2020), [arXiv:2002.02433 \[cond-mat.str-el\]](#).
- [49] Ting Fung Jeffrey Poon and Xiong-Jun Liu, “Quantum phase transition of fracton topological orders,” arXiv e-prints , arXiv:2001.05937 (2020), [arXiv:2001.05937 \[cond-mat.str-el\]](#).
- [50] Meng-Yuan Li and Peng Ye, “Fracton physics of spatially extended excitations,” *Phys. Rev. B* **101**, 245134 (2020).
- [51] Jian-Keng Yuan, Shuai A. Chen, and Peng Ye, “Fractonic superfluids,” *Physical Review Research* **2**, 023267 (2020), [arXiv:1911.02876 \[cond-mat.str-el\]](#).
- [52] Shuai A. Chen, Jian-Keng Yuan, and Peng Ye, “Fractonic superfluids. ii. condensing subdimensional particles,” *Phys. Rev. Research* **3**, 013226 (2021).
- [53] Hongchao Li and Peng Ye, “Higher Rank Symmetry and Angular Moment Conservation as Emergent Phenomena,” (2021), [arXiv:2104.03237 \[cond-mat.quant-gas\]](#).
- [54] Juven Wang and Shing-Tung Yau, “Non-Abelian gauged fracton matter field theory: Sigma models, superfluids, and vortices,” *Physical Review Research* **2**, 043219 (2020), [arXiv:1912.13485 \[cond-mat.str-el\]](#).
- [55] Tian Lan, Liang Kong, and Xiao-Gang Wen, “Classification of $(3+1)$ D bosonic topological orders: The case when pointlike excitations are all bosons,” *Phys. Rev. X* **8**, 021074 (2018).
- [56] Tian Lan and Xiao-Gang Wen, “Classification of $3+1$ D bosonic topological orders (ii): The case when some pointlike excitations are fermions,” *Phys. Rev. X* **9**, 021005 (2019).
- [57] AtMa P. O. Chan, Peng Ye, and Shinsei Ryu, “Braiding with borromean rings in $(3+1)$ -dimensional spacetime,” *Phys. Rev. Lett.* **121**, 061601 (2018).
- [58] Xueda Wen, Huan He, Apoorv Tiwari, Yunqin Zheng, and Peng Ye, “Entanglement entropy for $(3+1)$ -dimensional topological order with excitations,” *Phys. Rev. B* **97**, 085147 (2018).
- [59] Chenjie Wang and Michael Levin, “Braiding statistics of loop excitations in three dimensions,” *Phys. Rev. Lett.* **113**, 080403 (2014).
- [60] Chao-Ming Jian and Xiao-Liang Qi, “Layer construction of 3d topological states and string braiding statistics,” *Phys. Rev. X* **4**, 041043 (2014).
- [61] Shenghan Jiang, Andrej Meszaros, and Ying Ran, “Generalized modular transformations in $(3+1)$ D topologically ordered phases and triple linking invariant of loop braiding,” *Phys. Rev. X* **4**, 031048 (2014).
- [62] Chenjie Wang, Chien-Hung Lin, and Michael Levin, “Bulk-boundary correspondence for three-dimensional symmetry-protected topological phases,” *Phys. Rev. X* **6**, 021015 (2016).
- [63] Yidun Wan, Juven C. Wang, and Huan He, “Twisted gauge theory model of topological phases in three dimensions,” *Phys. Rev. B* **92**, 045101 (2015).
- [64] Peng Ye, Taylor L. Hughes, Joseph Maciejko, and Eduardo Fradkin, “Composite particle theory of three-dimensional gapped fermionic phases: Fractional topological insulators and charge-loop excitation symmetry,” *Phys. Rev. B* **94**, 115104 (2016).
- [65] Peng Ye and Zheng-Cheng Gu, “Topological quantum field theory of three-dimensional bosonic abelian-symmetry-protected topological phases,” *Phys. Rev. B* **93**, 205157 (2016).
- [66] A. Kapustin and R. Thorngren, “Anomalies of discrete symmetries in various dimensions and group cohomology,” ArXiv e-prints (2014), [arXiv:1404.3230 \[hep-th\]](#).
- [67] Peng Ye and Xiao-Gang Wen, “Constructing symmetric topological phases of bosons in three dimensions via fermionic projective construction and dyon condensation,” *Phys. Rev. B* **89**, 045127 (2014).
- [68] Shang-Qiang Ning, Zheng-Xin Liu, and Peng Ye, “Symmetry enrichment in three-dimensional topological phases,” *Phys. Rev. B* **94**, 245120 (2016).
- [69] S.-Q. Ning, Z.-X. Liu, and P. Ye, “Topological gauge theory, symmetry fractionalization, and classification of symmetry-enriched topological phases in three dimensions,” arXiv e-prints (2018), [arXiv:1801.01638 \[cond-mat.str-el\]](#).
- [70] Peng Ye, “Three-dimensional anomalous twisted gauge theories with global symmetry: Implications for quantum spin liquids,” *Phys. Rev. B* **97**, 125127 (2018).
- [71] Juven C. Wang and Xiao-Gang Wen, “Non-abelian string and particle braiding in topological order: Modular $SL(3, \mathbb{Z})$ representation and $(3+1)$ -dimensional twisted gauge theory,” *Phys. Rev. B* **91**, 035134 (2015).
- [72] Juven C. Wang, Zheng-Cheng Gu, and Xiao-Gang Wen, “Field-theory representation of gauge-gravity symmetry-protected topological invariants, group cohomology, and beyond,” *Phys. Rev. Lett.* **114**, 031601 (2015).
- [73] Xiao Chen, Apoorv Tiwari, and Shinsei Ryu, “Bulk-boundary correspondence in $(3+1)$ -dimensional topological phases,” *Phys. Rev. B* **94**, 045113 (2016).
- [74] Juven Wang, Xiao-Gang Wen, and Shing-Tung Yau, “Quantum statistics and spacetime surgery,” *Physics Letters B* **807**, 135516 (2020).
- [75] Pavel Putrov, Juven Wang, and Shing-Tung Yau, “Braiding statistics and link invariants of bosonic/fermionic topological quantum matter in $2+1$ and $3+1$ dimensions,” *Annals of Physics* **384**, 254 – 287 (2017).
- [76] Peng Ye, Meng Cheng, and Eduardo Fradkin, “Fractional s -duality, classification of fractional topological insulators, and surface topological order,” *Phys. Rev. B* **96**, 085125 (2017).
- [77] Apoorv Tiwari, Xiao Chen, and Shinsei Ryu, “Wilson operator algebras and ground states of coupled BF theories,” *Phys. Rev. B* **95**, 245124 (2017).
- [78] Kevin Walker and Zhenghan Wang, “ $(3+1)$ -TQFTs and topological insulators,” *Frontiers of Physics* **7**, 150–159 (2012), [arXiv:1104.2632 \[cond-mat.str-el\]](#).
- [79] Zhi-Feng Zhang and Peng Ye, “Compatible braidings with hopf links, multiloop, and borromean rings in $(3+1)$ -dimensional spacetime,” *Phys. Rev. Research* **3**, 023132 (2021).
- [80] Zhi-Feng Zhang and Peng Ye, “Topological Orders, Braiding Statistics, and Mixture of Two Types of Twisted BF Theories in Five Dimensions,” (2021), [arXiv:2104.07067 \[hep-th\]](#).
- [81] Yang Qiu and Zhenghan Wang, “Ground subspaces of topological phases of matter as error correcting codes,”

- Annals of Physics* **422**, 168318 (2020), [arXiv:2004.11982 \[quant-ph\]](#).
- [82] Sagar Vijay, “Isotropic Layer Construction and Phase Diagram for Fracton Topological Phases,” [arXiv e-prints](#), [arXiv:1701.00762](#) (2017), [arXiv:1701.00762 \[cond-mat.str-el\]](#).
 - [83] Han Ma, A. T. Schmitz, S. A. Parameswaran, Michael Hermele, and Rahul M. Nandkishore, “Topological entanglement entropy of fracton stabilizer codes,” *Phys. Rev. B* **97**, 125101 (2018).
 - [84] D. Hardorp, *All Compact Orientable Three Dimensional Manifolds Admit Total Foliations*, American Mathematical Society: Memoirs of the American Mathematical Society (American Mathematical Society, 1980).
 - [85] Wilbur Shirley, Kevin Slagle, and Xie Chen, “Foliated fracton order in the checkerboard model,” *Phys. Rev. B* **99**, 115123 (2019).
 - [86] Frank Schindler, Ashley M. Cook, Maia G. Vergniory, Zhijun Wang, Stuart S. P. Parkin, B. Andrei Bernevig, and Titus Neupert, “Higher-order topological insulators,” *Science Advances* **4**, eaat0346 (2018), [arXiv:1708.03636 \[cond-mat.mes-hall\]](#).
 - [87] Meng-Yuan Li and Peng Ye, unpublished.